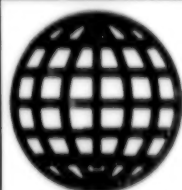


JFRS-UMS-93-005
6 August 1993



**FOREIGN
BROADCAST
INFORMATION
SERVICE**

JPRS Report

Science & Technology

***Central Eurasia:
Materials Science***

Science & Technology

Central Eurasia: Materials Science

JPRS-UMS-93-005

CONTENTS

6 August 1993

ANALYSIS, TESTING

Investigation of Patterns of Ti-Co Pig Iron Atomization by Nitrogen [Ye.L. Muravyeva, S.Yu. Filatova, et al.; <i>METALLY</i> , No 3, May-Jun 93]	1
Deuterium Accumulation in Titanium During Implantation [V.L. Arbuzov, V.B. Vykhodets, et al.; <i>METALLY</i> , No 3, May-Jun 93]	1
Anomalous Properties of UNi ₃ -UCu ₃ Solid Solutions [G.I. Terekhov, S.I. Sinyakova; <i>METALLY</i> , No 3, May-Jun 93]	1
Thermoelectric Signals in Shock Wave Compression of a Semiconductor Specimen in a Flat Conservation Experiment Container [S. S. Nabatov, A. V. Lebedev; <i>KHIMICHESKAYA FIZIKA</i> , Feb 93]	1
Behavior of Composite Materials under High Stretching Rates (Cleavage) [V. A. Ogorodnikov, V. I. Luchinin, et al.; <i>KHIMICHESKAYA FIZIKA</i> , Feb 93]	2
Deposition of Carbide Coatings by Means of Vapor-Phase Transfer Self-Propagating High-Temperature Synthesis Reactions [Yu. A. Shvetsov, E. A. Shtessel, et al.; <i>KHIMICHESKAYA FIZIKA</i> , Feb 93]	2
Gasless Detonation in Processes of Explosive Decomposition of Azides of Heavy Metals [V. V. Barelko, S. M. Ryabikh, et al.; <i>KHIMICHESKAYA FIZIKA</i> , Feb 93]	2
Kinetics of Formation of Isothermal Supersaturated Vapor Phase in the System GaAs-GaP-AsCl ₃ -H ₂ [I.V. Antonov, S.K. Guba, et al.; <i>NEORGANICHESKIYE MATERIALY</i> , Feb 93]	2
Effect of Laser Irradiation on Optical Properties of Heteroepitaxial ZnSe/GaAs(100) [A.V. Kovalenko, A.Yu. Mekekechko, et al.; <i>NEORGANICHESKIYE MATERIALY</i> , Feb 93]	3
Thermoelectric Properties of Single Crystals of the System Bi ₂ Te ₃ -Sb ₂ Te ₃ -Bi ₂ Se ₃ [L. D. Ivanova, Yu. V. Granatkina; <i>NEORGANICHESKIYE MATERIALY</i> , Feb 93]	3

COATINGS

Powders of the System xAl ₂ O ₃ -yTiO ₂ for Plasma-Torch Spraying [G.V. Lavrova, S.V. Milovzorova, et al.; <i>POROSHKOVAYA METALLURGIYA</i> , Jan 93]	4
Formation of Nickel-Doped Chromium Coatings on Diamond [V.G. Chuprina, I.M. Shalya, et al.; <i>POROSHKOVAYA METALLURGIYA</i> , Jan 93]	4
Long-Range Interaction Effect Under Ionic Irradiation of Metal Foils [P.V. Pavlov, D.I. Tetelbaum, et al.; <i>METALLY</i> , No 3, May-Jun 93]	4
Diffusion Mechanisms and Stability of Properties of Thin-Film Ti-Ni-Au, W-Ni-Au, and Mo-Ni-Au Systems on Silicon [T.V. Litvinova, Yu.N. Makogon, et al.; <i>METALLY</i> , No 3, May-Jun 93]	5
Optimizing the Composition of Deposited Metal and Parameters of Wear-Resistant Buildup Techniques [L. S. Livshits, O. Yu. Yelagina; <i>SVAROCHNOYE PROIZVODSTVO</i> , Aug 92]	5
Laser Technology for Imparting Tribotechnical Characteristics to Friction Surfaces [V. S. Avanesov; <i>SVAROCHNOYE PROIZVODSTVO</i> , Aug 92]	5
Modification of the Surface Layer of Parts by Micro-Arc Oxidation [V. A. Fedorov; <i>SVAROCHNOYE PROIZVODSTVO</i> , Aug 92]	6
Wear Resistance of Coatings Based on Metalide Alloys [V. A. Neuymin, S. A. Shelukha, et al.; <i>SVAROCHNOYE PROIZVODSTVO</i> , Aug 92]	6
Structure and Properties of Coatings Applied with a CO ₂ Laser [V. Ye. Arkhipov, A. A. Ablayev, L. T. Krasnov; <i>METALLOVEDENIYE I TERMICHESKAYA OBRABOTKA METALLOV</i> , Jul 92]	6

CORROSION

Corrosion Resistance of Tubular Parts Coated With Z-Al Alloy [Ye.V. Proskurkin, I.Ye. Mitnikov, et al.; <i>ZASHCHITA METALLOV</i> , Vol 29 No 1, Jan-Feb 93]	7
Electrolyte for Deposition of Ni-Teflon Composite Coatings [N.M. Teterina, G.V. Khaldeyev; <i>ZASHCHITA METALLOV</i> , Vol 29 No 1, Jan-Feb 93]	7
Approximate Design of Potential Transducers for Inspecting Electrochemical Protection of Underground Steel Pipes [L.I. Freyman; <i>ZASHCHITA METALLOV</i> , Vol 29 No 1, Jan-Feb 93]	7

Atmospheric Corrosion of Metals and Alloys in "Mirny" Station in Antarctica [A.A. Mikhailov, Yu.N. Mikhailovskiy, et al.; ZASHCHITA METALLOV, Vol 29 No 1, Jan-Feb 3]	8
Estimating Corrosion Resistance of Welded Ti-Alloy Joints by Polarization Resistance Method [S.G. Polyakov, G.M. Grigorenko, et al.; ZASHCHITA METALLOV, Vol 29 No 1, Jan-Feb 93]	8
The Effect of Molybdenum Content on Intercrystalline Corrosion in KhN40MDB Alloy [E. T. Shapovalov and M. Yu. Ustimenko; ZASHCHITA METALLOV Vol 29, No 2, Mar-Apr 1993]	9
Durability of Corrosion-Resistance Polymer Coatings for the External Surfaces of Underground Pipelines [Yu. I. Garber; ZASHCHITA METALLOV Vol 29, No 2, Mar-Apr 1993]	9

FERROUS METALS

Behavior Characteristics of Physical Properties of VNL Steels in Liquid State [L.A. Oborin, Ye.Ye. Tretyakova, et al.; METALLY, No 3, May-Jun 93]	10
Structurization of Grain-Oriented Electric Steel During Annealing in Various Atmospheres [A.G. Dukhnov, A.M. Chernykh, et al.; STAL, No 1, Jan 93]	10
Continuous Casting of 12Cr18Ni10Ti Steel in Horizontal MNLZ Casting Machine with Bilateral Extraction of Ingot without Scarfing of Cast Metal [A.M. Chigrinov, V.M. Parshin, et al.; STAL, Jan 93]	10
Structural and Technological Prerequisites for Producing New Generation of Grain-Oriented Electrical Sheet Steel [G.A. Brashevan, M.M. Borodkina, et al.; STAL, Jan 93]	11
Electrical Steels with High Silicon Content [A.P. Khomskiy; STAL, Jan 93]	12

NONFERROUS METALS, ALLOYS, BRAZES, SOLDERS

Resource Conservation and Improvement of Nickel-Based Superalloy Casting Performance by High-Temperature Melt Treatment [B.A. Baum, V.N. Larionov, et al.; METALLY, No 1, Jan-Feb 93]	13
Mixing Volume Correlation of Binary and Ternary Ni-Fe-Mo Alloys [V.V. Leonov, G.A. Nikiforov, et al.; METALLY, No 1, Jan-Feb 93]	13
On Issue of Dendritic Inhomogeneity in Single Crystal Ingots From YuNDKT5AA Alloy Grown at Various Rates [I.V. Belyayev, M.V. Pikunov, et al.; METALLY, No 1, Jan-Feb 93]	13
On Martensitic Transformations in Fe- and U-Based Alloys [A.N. Kobylkin, A.G. Nikolayev, et al.; METALLY, No 1, Jan-Feb 93]	14
Investigation of Surface Layer's Chemical Composition and Diffusion Processes in Cu-Ni-Au System [S.I. Sidorenko, T.V. Litvinova, et al.; METALLY, No 1, Jan-Feb 93]	14
Radiation-Induced Processes in Metallic Alloys' Subsurface Layers [G.G. Bondarenko; METALLY, No 1, Jan-Feb 93]	14
New Compounds With YbMo ₂ Al ₄ and Th ₂ Zn ₁₇ Structure [B.M. Stelmakhovich, Yu.B. Kuzma, et al.; METALLY, No 1, Jan-Feb 93]	14

PREPARATIONS

Electrochemical Synthesis of Tungsten and Molybdenum Borides in a Disperse State [Kh.B. Kushkhov, V.V. Malyshev, et al.; POROSHKOVAYA METALLURGIYA, Jan 93]	16
Calculating Compaction Kinetics of Powder Amorphous Metal Materials in the Process of Hot Isostatic Compaction [V.A. Posdnyakov, V.Ye. Vaganov; POROSHKOVAYA METALLURGIYA, Jan 93]	16
The Structure and Properties of Iron-Based Alloys Sintered by the Method of Electrocontact Heating [L.O. Andurshchik, E. Dudrova, et al.; POROSHKOVAYA METALLURGIYA, Jan 93]	16
Magnesium-Phosphate Self-Hardening Sands [S. I. Rivkin, Ye. N. Yurginson, L. G. Sudakas, L. I. Turkina; LITEYNOYE PROIZVODSTVO, Jun 92] ...	17
Quality of Sand from Tolmachevo Evaluated [Yu. F. Borovskiy, I. V. Shergin, Yu. N. Zinin; LITEYNOYE PROIZVODSTVO, Jun 92]	17
Making Casting Molds Using Vibration Methods [A. A. Brechko, A. V. Sokolov; LITEYNOYE PROIZVODSTVO, Jun 92]	17
Casting of Aluminum-Based Composites With Crystallization Under Pressure [N. N. Belousov; LITEYNOYE PROIZVODSTVO, Jun 92]	18
Making Castings of Metal-Base Composites [V. G. Borisov; LITEYNOYE PROIZVODSTVO, Jun 92] ..	18
Ceramic Molds for Relief Surface Castings [F. D. Obolentsev, Yu. A. Kaplunovskiy, L. M. Mirson; LITEYNOYE PROIZVODSTVO, Jun 92]	18
Combined Method of Manufacturing Gas Turbine Rings [A. G. Kovalev, A. N. Lemeshko, N. V. Levnikov; LITEYNOYE PROIZVODSTVO, Jun 92]	18

Doping $\text{Bi}_2\text{Te}_{2.85}\text{Se}_{0.15}$ Solid Solution with Tellurides of Yttrium (Y_2Te_3) and Gadolinium (Gd_2Te_3) [T. Ye. Svechnikova, S. N. Chizhevskaya, et al.; NEORGANICHESKIYE MATERIALY, Feb 93]	19
Production and Properties of $\text{Ag}_{0.12}\text{Ga}_{0.12}\text{Ge}_{0.88}\text{Se}_2$ Single Crystal [I.D. Oleksyuk, G. Ye. Davidiuk, et al.; NEORGANICHESKIYE MATERIALY, May 93]	19
Electronic Structure and Optical Properties of ZrO_2 stabilized with Yttrium [G.A. Olkhovik, I.I. Naumov, et al.; NEORGANICHESKIYE MATERIALY, May 93]	20
Determining Possibility of Superconductivity in $\text{La}_{2-x}(\text{M}^{2+} = \text{Ca}, \text{Sr}, \text{Ba})_x\text{Cu}_2\text{O}_6$ on Basis of Their Electronic Structure [V.P. Zhukov; NEORGANICHESKIYE MATERIALY, May 93]	20
Possibility of Cold Nuclear Fusion at Temperature of Ferroelectric Phase Transition in KD_2PO_4 [V.B. Kalinin; NEORGANICHESKIYE MATERIALY, May 93]	20
Chemical Structure Specifics and Optical Properties of Sulfur-Enriched As-S-Ge Glasses [D.I. Tsiulyanu, N.A. Gumenyuk; NEORGANICHESKIYE MATERIALY, May 93]	21
Mechanism of $\text{YBa}_2\text{Cu}_3\text{O}_{7-x}$ and $\text{Ca}_2\text{Sr}_2\text{Bi}_2\text{Cu}_3\text{O}_{10-x}$ by Nitrogen Oxides according to Electron-Paramagnetic Resonance Data [E.F. Saakyan, A.A. Muradyan, et al.; NEORGANICHESKIYE MATERIALY, May 93]	21
Solid Solution $\text{Y}_{1-x}\text{Ln}_x\text{Ba}_2\text{Cu}_3\text{O}_{7-y}$ ($\text{Ln} = \text{Ce}, \text{Pr}, \text{Tb}$) [V.V. Zelentsov, T.N. Fesenko, et al.; NEORGANICHESKIYE MATERIALY, May 93]	21

TREATMENTS

Effect of Electrohydropulse Treatment (EGIO) on Metallic Melt Properties [G.S. Yershov, V.I. Klichanovskiy, et al.; METALLY, No 3, May-Jun 93]	23
Oxidized Metal and Alloy Behavior Characteristics Under Electron Bombardment Conditions [G.G. Bondarenko, A.P. Korzhavyy, et al.; METALLY, No 3, May-Jun 93]	23
Radiation Heat Treatment of Steel [Yu.I. Gofman; METALLY, No 3, May-Jun 93]	23
Effect of Heat Treatment on Uniform Elongation of Medium Carbon Steel [A. A. Azarkevich, A. A. Pashchenko, T. A. Yevtukhova; METALLOVEDENIYE I TERMICHESKAYA OBRABOTKA METALLOV, Jul 92]	23
Oxidation of Pipe During Combined Furnace and Induction Heating [A. A. Zgura, O. T. Nikolskaya, T. V. Ivanova, I. S. Stefanskiy; METALLOVEDENIYE I TERMICHESKAYA OBRABOTKA METALLOV, Jul 92]	24
Electron Beam Treatment of Bearing Steels [A. A. Shulga; METALLOVEDENIYE I TERMICHESKAYA OBRABOTKA METALLOV, Jul 92]	24
Effect of the Content of Alloying Elements in Different Grades of Alloy KhN65KVMYuTB on Its High-Temperature Strength [M. A. Filatova, V. S. Sudakov, I. V. Kabanov; METALLOVEDENIYE I TERMICHESKAYA OBRABOTKA METALLOV, Jul 92]	25
Deformation Waves Near Nonmetallic Inclusions in Explosive Working of Metals [S. I. Gubenko; METALLOVEDENIYE I TERMICHESKAYA OBRABOTKA METALLOV, Jul 92]	25
Niobium's Effect on the Structure of Chromium Ferritic Steel [G. A. Burakova, Ye. K. Koval, et al.; METALLOVEDENIYE I TERMICHESKAYA OBRABOTKA METALLOV, Jul 92]	25
Nature of the Internal Friction Peak in Beryllium at 100-200°C [G. F. Tikhinskiy, I. I. Papirov, et al.; METALLOVEDENIYE I TERMICHESKAYA OBRABOTKA METALLOV, Jul 92]	26

WELDING, BRAZING AND SOLDERING

Computer Simulation in Determining Weldability and Selecting Welding Parameters for Steels and Alloys [A. N. Khakimov; SVAROCHNOYE PROIZVODSTVO, Aug 92]	27
Resistance of Gas Mains to Propagation of Extended Continuous Fractures [G. I. Makarov; SVAROCHNOYE PROIZVODSTVO, Aug 92]	27
Higher Durability for Large Welded Metalwork Subject to Corrosive Environments of the Oil and Gas Industry [A. I. Korolev, A. V. Muradov; SVAROCHNOYE PROIZVODSTVO, Aug 92]	27
Effect of Laser Treatment on Corrosion Resistance of Steels and Welds [R. D. Radchenko; SVAROCHNOYE PROIZVODSTVO, Aug 92]	27

Investigation of Patterns of Ti-Co Pig Iron Atomization by Nitrogen

937D0112C Moscow METALLY in Russian No 3, May-Jun 93 pp 21-24

[Article by Ye.L. Muravyeva, S.Yu. Filatova, Ye.Ye. Baryshev, Yekaterinburg; UDC 621.762]

[Abstract] Production of metal powders by atomizing the melt jet with a gas flow and ways of controlling the process are discussed, and it is noted that known patterns do not always hold true for multiphase composition due to the presence of surfactants, which lead to the appearance of extrema on the surface tension curves, and the melt heterogeneity, which affects the temperature dependence of viscosity. To clarify the situation, the patterns of multicomponent alloy atomization are examined, and an attempt is made to find the correlation between the particle parameters and melt properties. To this end, the patterns of Ti-Cu pig iron (TU-14-15-219-89) atomization by 99.8% pure nitrogen are studied. The effect of the melt temperature prior to atomization on the granulometric composition of the powder, i.e., the mean particle diameter and the particle size distribution, is analyzed. The alloy is melted and atomized in a sealed atomization unit designed by the Metallurgy Institute at the Urals Department of Russia's Academy of Sciences. The unit design and the alloy composition are summarized. The integral particle size distribution curves and the dependence of the alloy mean particle size, surface tension, density, and viscosity are plotted. A model for calculating the mean particle size is proposed. The findings demonstrate that the melt properties have a definitive effect on the granulometric composition, especially the mean particle size. It is stressed that an analysis of the atomized alloy properties and a search for ways of controlling them are indispensable for predicting the granulometric characteristics of the resulting powder. Figures 3; references 7: 5 Russian, 2 Western.

Deuterium Accumulation in Titanium During Implantation

937D0112E Moscow METALLY in Russian No 3, May-Jun 93 pp 93-96

[Article by V.L. Arbuzov, V.B. Vykhodets, S.M. Klotsman, V.A. Pavlov, G.A. Raspopova, Yekaterinburg; UDC 621.039.53:669.783]

[Abstract] Interest in the hydrogen isotope distribution in irradiated metal samples, e.g., reactor core walls, and earlier studies of D accumulation in V-D alloys are discussed, and it is speculated that enrichment in D depends on its concentration in the alloy and is due to D atom capture by radiation-induced defects resulting in the formation of low-mobility defect-D centers. The study is continued with Ti, and the D accumulation is studied in samples of single crystal Ti with less than 500 ppm of interstitial impurities, polycrystalline pure Ti, and a Ti alloy with 6% Al and 0.2% O₂. A nuclear

microanalysis employing the D(d, p)T reaction reveals that the implanted D accumulates less in the irradiated volume of Ti than one would expect on the basis of published data on thermal diffusion in the Ti-D system. It is speculated that this is due to the accelerated radiation-induced D diffusion in Ti. The study shows that at a D energy of 17 and 700 keV, implantation does not lead to noticeable surface layer enrichment in D. Figures 1; references 8: 5 Russian, 3 Western.

Anomalous Properties of UNi₅-UCu₅ Solid Solutions

937D0112I Moscow METALLY in Russian No 3, May-Jun 93 pp 237-239

[Article by G.I. Terekhov, S.I. Sinyakova, Moscow; UDC 54-165]

[Abstract] The lack of published data on the properties of solid solutions of pseudobinary metal systems synthesized from intermetallic compounds prompted a study of continuous series of solid solutions formed by fusing UNi₅-Cu₅ compounds. The behavior of the crystal lattice parameters, electric resistivity, and hardness within the entire range of concentrations as a function of composition are examined. The alloy and compound preparation procedures are outlined, and the behavior of the crystal lattice spacing, hardness, and resistivity in solid solutions of UNi₅-UCu₅ is plotted. The X-ray diffraction study is conducted by Debye's method using unfiltered FeK radiation. The electric resistance is measured by the potentiometric method using a galvanometer and potentiometer. The series of solid solutions under study displays a number of abnormal properties despite the anticipated patterns of their behavior; it is speculated that the anomalies are not related to the formation of new phases but have a different origin. The conclusion that the continuous series of solid solutions may not follow the rule of gradual change in properties has far-reaching implications. It is noted that when intermetallic compounds are fused with isomorphous BCC lattices, a sharp change in the lattice constant is also observed. Figures 1; references 3: 2 Russian, 1 Western.

Thermoelectric Signals in Shock Wave Compression of a Semiconductor Specimen in a Flat Conservation Experiment Container

937D0101A Moscow KHIMICHESKAYA FIZIKA in Russian Vol 12 No 2, Feb 93 pp 167-169

[Article by S. S. Nabatov and A. V. Lebedev, Institute of Chemical Physics, Russian Academy of Sciences, Chernogolovka]

[Abstract] Thermoelectric signals were recorded in a conservation experiment with shock wave compression of a semiconductor specimen in a steel box. A p-type semiconductor material, stannous sulfide compressed to a density of 4.5 g/cm³, was placed in the steel box with a wall thickness of 7 mm on the side receiving the shock

wave. A pressure pulse of 16 GPa was generated in the steel by an aluminum striker 5 mm thick and 90 mm in diameter. Results of the experiment indicate that the appearance of thermoelectric signals (in the relieved state of the specimen) is due to uneven heating of the specimen as a result of plastic deformation of the box. A negative signal indicates that the strongest heating takes place at the surface of the rear wall of the box (away from the shock wave).

Behavior of Composite Materials under High Stretching Rates (Cleavage)

937D0101B Moscow *KHIMICHESKAYA FIZIKA* in Russian Vol 12 No 2, Feb 93 pp 178-179

[Article by V. A. Ogorodnikov, V. I. Luchinin, Ye. S. Tyunkin, V. A. Grigoryev, A. P. Tsoy, and A. A. Khokhlov]

[Abstract] Cleavage under high stretching rates was investigated in two types of composite materials: VNZh-95, which consists of 95 wt.% W, 1.5 wt.% Ni, and 3.5 wt.% Fe, and VNKd-80, which consists of 80 wt.% W, 1 wt.% Ni, and 19 wt.% Cd. Specimens' resistance to cleavage was determined in two types of experiments. In the first type, the loading conditions had a shock wave pressure profile that was nearly rectangular in shape. In the second type, the loading conditions had a shock wave pressure profile that was nearly triangular in shape.

It was found that the composite materials' resistance to cleavage has only a slight dependence on the intensity of the shock wave. Metallographic analysis of the specimens (after their loading to the point where centers of failure appear) in both types of experiments showed that for VNZh-95, centers of failure in the form of micropores and microcracks appear and become united only between tungsten grains, and for VNKd-80, centers of failure appear as micropores that form in cadmium, which has comparatively low strength, and become united in the form of microcracks along inclusions of cadmium between tungsten grains.

Deposition of Carbide Coatings by Means of Vapor-Phase Transfer Self-Propagating High-Temperature Synthesis Reactions

937D0101C Moscow *KHIMICHESKAYA FIZIKA* in Russian Vol 12 No 2, Feb 93 pp 260-267

[Article by Yu. A. Shvetsov, E. A. Shtessel, D. Yu. Kovalev, Ye. P. Kostogorov, A. A. Shirayev, T. I. Yanson, and N. B. Manyako, Institute of Structural Macrokinetics, Russian Academy of Sciences, Moscow, and Lvov State University; UDC 621.793.669.586]

[Abstract] Results are presented of studies on the use of the new technique of vapor-phase transfer, self-propagating, high-temperature synthesis reactions for depositing carbide coatings on metals. Experiments were conducted to determine conditions of formation, structure, phase composition and properties of chromium

carbide coatings deposited by this technique, and the results are reported and discussed. Data indicate that the technique also has prospects for carburization and related processes that compare advantageously with existing diffusion carburization methods in that it is possible to case-harden metal products directly in the self-propagating, high-temperature synthesis process, meaning with less time and energy expended.

Gasless Detonation in Processes of Explosive Decomposition of Azides of Heavy Metals

937D0101D *KHIMICHESKAYA FIZIKA* in Russian Vol 12 No 2, Feb 93 pp 274-282

[Article by V. V. Barelko, S. M. Ryabykh, and K. Sh. Karabukayev, Institute of Chemical Physics, Russian Academy of Sciences, Chernogolovka; UDC 662.215.4]

[Abstract] Dynamic features of explosive decomposition of single crystals of silver and lead azides were investigated. The experiment set-up involved specially grown crystals in whisker form, a high-energy electron beam to initiate the explosive decomposition process, and high-speed optical recording devices, which permitted analysis of the explosion process in the nanosecond time-frame and examination of stage and phase peculiarities of detonation. It was found that the explosion process contains two sequential stages of a detonation character and that the first of them can be interpreted as a gasless detonation stage. It is pointed out that this conclusion should remain a hypothesis pending further experimental and theoretical substantiation.

Kinetics of Formation of Isothermal Supersaturated Vapor Phase in the System GaAs-GaP-AsCl₃-H₂

937D0095A Moscow *NEORGANICHESKIYE MATERIALY* in Russian Vol 29 No 2, Feb 93 pp 174-176

[Article by I. V. Antonov, S. K. Guba, Yu. V. Zhilyayev, V. V. Zelenin, and A. Yu. Kulikov, A. F. Ioffe Physical-Technical Institute, Russian Academy of Sciences; UDC 541.123.7]

[Abstract] Temperature dependences were determined for rates of chemical reactions taking place when GaAs and GaP are used as sources for chloride vapor phase epitaxy. Experiments were conducted in a quartz container with the same geometric parameters as the source zone of a standard horizontal reactor. In the investigated range of temperatures (840-1070 K) and flow rates, the diffusion length of any of the reactants during the time of contact of vapor and solid phases was large in comparison with the height of the channel (0.3 cm) and small in comparison with the length of the source (6 cm). This made it possible to exclude diffusion flows and spatial distribution of component concentrations from consideration and to limit the study to a one-dimensional approximation for a system of first-order differential

equations of continuity. It was found that in the system GaP-AsCl₃-H₂ in a temperature range of 870-970 K, it is possible to create a supersaturated vapor phase and grow epitaxial layers of solid GaAs_{1-x}P_x ($x \leq 0.75$) in isothermal conditions.

Effect of Laser Irradiation on Optical Properties of Heteroepitaxial ZnSe/GaAs(100)

937D0095B Moscow NEORGANICHESKIYE
MATERIALY in Russian Vol 29 No 2,
Feb 93 pp 183-186

[Article by A. V. Kovalenko and A. Yu. Mekechko, Dnepropetrovsk State University, and P. Lilley, University of Manchester; UDC 539.216.2]

[Abstract] Optical properties of heteroepitaxial ZnSe on a GaAs(100) substrate were investigated for two different types: ones produced by conventional vapor phase epitaxy (VPE) and ones produced by photo-assisted vapor phase epitaxy (PAVPE). Both types were grown in a computer-controlled unit with identical growing process parameters. Photoluminescence and reflection spectra and morphology characteristics of heteroepitaxial ZnSe/GaAs(100) produced by PAVPE were compared with those of VPE specimens. It was found that when treated with an He-Ne laser ($h\nu \approx 2$ eV), the epilayer's surface and optical properties were not different. When a He-Cd laser ($h\nu \approx 2.807$ eV) with an

energy of photons exceeding that of the forbidden band of ZnSe was used, improvement in morphology (mirror-like quality of the surface) was noted as well as increased radiation intensity of free and bound excitons in the photoluminescence spectrum.

Thermoelectric Properties of Single Crystals of the System Bi₂Te₃-Sb₂Te₃-Bi₂Se₃

937D0095D Moscow NEORGANICHESKIYE
MATERIALY in Russian Vol 29 No 2,
Feb 93 pp 193-196

[Article by L. D. Ivanova and Yu. V. Granatkina, A. Baykov Institute of Metallurgy, Russian Academy of Sciences; UDC 537.32]

[Abstract] The Czochralski process was used to grow single crystals of the system Bi₂Te₃-Sb₂Te₃ containing from 25 to 40 mol.% Bi₂Te₃ and doped with 2 and 4 mol.% Bi₂Se₃. The thermoelectromotive force coefficient and electric and thermal conductivity were measured at room temperature in specimens cut from single crystals of different compositions. It was found that as Bi₂Te₃ and Bi₂Se₃ content increased, the crystals' electric and thermal conductivity decreased, and the thermoelectromotive force coefficient increased. In thermocouples made of the crystals, the thermoelectric figure of merit was $(2.8-2.9) \times 10^{-3} \text{K}^{-1}$ at a heat transfer temperature of 303 K⁻¹.

Powders of the System $x\text{Al}_2\text{O}_3\text{-}y\text{TiO}_2$ for Plasma-Torch Spraying

937D0103E Kiev *POROSHKOVAYA METALLURGIYA* in Russian No 1, Jan 93 (manuscript received 5 Feb 91) pp 56-60

[Article by G.V. Lavrova, S.V. Milovzorova, I.V. Plyuto, and V.M. Beletskiy, General and Inorganic Chemistry Institute, Ukraine Academy of Sciences, Kiev; UDC 66.099.5; 621.793]

[Abstract] A study examined the possibility of producing $x\text{Al}_2\text{O}_3\text{-}y\text{TiO}_2$ composites by cladding titanium dioxide with aluminum dioxide from solutions. Hydrated titanium dioxide in amounts required to produce composites containing 3, 13, and 40% TiO_2 in relation to aluminum oxide in the end product was added to a solution of one of two systems: $\text{Al-NaOH-H}_2\text{O}$ (the solution was presaturated with sodium aluminate) or $\text{Al}_{\text{act}}\text{-H}_2\text{O}$ (the aluminum's surface was preplated with a molten metal film). The sediment was separated from the solution, dried, and baked. Their physicochemical properties were studied by roentgenography, infrared spectroscopy, granulometry, photoelectric spectroscopy, and thermal analysis by using the following pieces of equipment: DRON-3, UR-10, SK Lazer raikron sayzer, VIEE-15, and KVDS-2800. The powders produced from the first of the above systems were found to be spheroidized and represent the sum of metal oxides in polymorphous form dictated by the heat treatment temperature. Their physical properties depended on the baking temperature. Their maximum specific surface ($210 \text{ m}^2/\text{g}$) was obtained at heat treatment temperatures of $500\text{-}700^\circ\text{C}$ with $\gamma\text{-Al}_2\text{O}_3$ as the primary phase. Two specimens synthesized on the basis of the first system were analyzed. Polymorphous transformation of the α - and β -form of $\text{Al}_2\text{O}_3 \times \text{TiO}_2$ (at $1,820^\circ\text{C}$) occurred in only one of the two specimens. Its nucleus consisted of rutile clad with aluminum hydroxide. Titanium was present only in the center part of the particle. In the composites synthesized from the second system, titanium dioxide was clad only in an alkalized solution. Titanium dioxide was shown to function as a "seed" element solely from the surface of a particle because the nonuniform distribution of the absorbed cation (sodium) throughout the particle's volume occurring in the first stage of the exchange process is preserved in the rutile and afterward. In composites from which the alkaline solution had been rinsed off, the bond energy of the titanium's $2p_{3/2}$ electrons decreased to 1 eV. This was attributed to a donor-acceptor reaction with aluminum hydroxide. The experiments confirmed that it is possible to synthesize $x\text{Al}_2\text{O}_3\text{-}y\text{TiO}_2$ powders with a low-melting component (titanium dioxide) clad with aluminum hydroxide formed by oxidation of aluminum by water in alkaline solutions without having to use any grinding in the synthesis process. Figures 4, table 1; references 7; Russian.

Formation of Nickel-Doped Chromium Coatings on Diamond

937D0103D Kiev *POROSHKOVAYA METALLURGIYA* in Russian No 1, Jan 93 (manuscript received 18 Nov 91) pp 47-51

[Article by V.G. Chuprina, I.M. Shalya, and V.V. Shurkhal, Materials Science Problems Institute, Ukraine Academy of Sciences, Kiev; UDC 621.921.34.684.4.669.268]

[Abstract] X-ray phase analysis was used to study the structure formation processes occurring when nickel-doped chromium coatings are applied to diamond powders. At the annealing temperatures studied, adding NiO to chromium was found to reduce the thickness of the coatings formed on the diamond. As the process temperature was increased, the thickness of all the coatings tested increased. Their Cr and Cr_3C_2 contents increased as well. When nickel was used in amounts greater than 7.9%, the intensity of the reflexes from Ni(Cr) and Cr_2O_3 increased, whereas that from chromium decreased. This was explained in terms of the fact that the formation of chromium coatings is determined primarily by two processes: transfer of chromium to the reaction surface (diamond or coating) through the gas phase and diffusion of carbon from the diamond in the coating to this surface. The reaction of the carbon and chromium causes carbides to appear in the coating. If nickel monoxide is added to the metallizing agent (chromium powder), metallic nickel and Cr_2O_3 appear in the coating. The oxide blocks the vaporization of the chromium. The observed increase in coating thickness as the NiO content in the Mo + NiO metallizing mixture was increased was linked to the formation of the volatile oxide MoO_3 that is transferred through the gas phase and is the prime factor responsible for the increase in the thickness of Mo-Ni coatings. The studies also confirmed that nickel participates in the coating formation process. Increases in metallization temperature activate the processes dictating the appearance of nickel in the coating and facilitate the dissolution of chromium in its lattice. The presence of Ni(Cr) in the used metallizing agent indicated that not all of the reduced nickel is used to form the coating, however. Two factors were thus found to limit the growth of Ni-doped chromium coatings on diamond, i.e., Cr_2O_3 (which results from the reduction of NiO by chromium) and Ni(Cr) (which results from the dissolution of chromium in nickel). They are the main reasons for the decrease in coating thickness when nickel monoxide is added to a chromium metallizing agent. Tables 2; references 15; 14 Russian, 1 Western.

Long-Range Interaction Effect Under Ionic Irradiation of Metal Foils

937D0112D Moscow *METALLY* in Russian No 3, May-Jun 93 pp 78-83

[Article by P.V. Pavlov, D.I. Tetelbaum, Ye.V. Kurilchik, O.I. Kunitsyna, I.V. Tulina, Nizhny Novgorod; UDC 669.416+616-001.2]

[Abstract] The behavior of metal under irradiation, particularly the long-range interaction (ED) phenomenon, and the lack of a unified concept of the mechanism of this effect, as well as numerous models being proposed by various authors are discussed. An attempt is made to select the most plausible model. The patterns of the long-range interaction phenomenon in metal foils bombarded by ionic radiation are studied. Rolled Ni-Fe and Permalloy 18- μm -thick foils are irradiated; the ILU-3 accelerator is used to implant ions with a varying mass in a scanning mode at a mean ionic current density of 1 and $10 \mu\text{A}/\text{cm}^2$. To remove the layers, the foils are etched in an $\text{HNO}_3\text{:HF:H}_2\text{O}$ solution with a 2:1:5 ratio at a $0.1 \mu\text{m}/\text{min}$ rate. The microhardness is measured by a PTM-3 tester.

and the ultimate strength and Young modulus are measured by a 12 PM5/20-1 instrument. The dependence of the irradiated and nonirradiated foil side microhardness on the A⁺ and B⁺ dose at a 40 keV ion energy and 1 $\mu\text{m}/\text{cm}^2$ current density and the dependence of microhardness on the etched-off irradiated and nonirradiated layer thickness for the same ion energy and current density at a $6 \times 10^{13} \text{ cm}^{-2}$ are plotted. The behavior of the ultimate strength and effective modulus of elasticity under irradiation and the effect of film coats on the microhardness of exposed and unexposed foils are summarized. The dependence of microhardness on the ion energy and ion current density for exposed and unexposed foil sides, on the inert gas and chemically active element ion mass for the exposed and unexposed foil sides, as well as on the protective foil thickness are examined. The findings make it possible to identify the radiation-induced defects (vs. local heating) as the dominant source of elastic stress along the ion track. It is noted that the findings pose more questions than they answer yet create the conditions for further research. In all, the results point toward the validity of the wave model, whereby the elastic waves generated by the ion beam lead to a system of defects resulting in long-range interaction phenomena. Figures 5; tables 2; references 13: 12 Russian, 1 Western.

Diffusion Mechanisms and Stability of Properties of Thin-Film Ti-Ni-Au, W-Ni-Au, and Mo-Ni-Au Systems on Silicon

937D0112H Moscow METALLY in Russian No 3, May-Jun 93 pp 205-209

[Article by T.V. Litvinova, Yu.N. Makogon, S.I. Sidorenko, Kiev; UDC 669.548.55]

[Abstract] Microinstruments and thin-film metal elements, whose structure stability and operating reliability depend on our knowledge of the diffusion structure- and phase-formation under heat treatment and other thermal exposures, and the available data on processes that determine the structure and property stability of thin films under thermal exposure prompted an examination of the principles of structure and phase formation in Ti-Ni-Au, W-Ni-Au, and Mo-Ni-Au systems under the effect of heat treatment. An experimental study is carried out to ascertain the mechanisms responsible for the temperature-time stability intervals of these systems' structure and properties. The 2% resistivity variation level under various thermal exposures is used as the stability criterion. The mechanical stress, grain size, crystal lattice constants of the Ni and Au layers, the electrophysical properties, phase formation, mass transport in the systems, and heat treatment in the air up to 500 h long in the air at a temperature of up to 650K are examined. The multilayer Ti-Ni-Au, W-Ni-Au, and Mo-Ni-Au systems are formed by successive deposition onto a single crystal KES-01 Si(111) substrate. The findings show that the Ti-Ni-Au systems have the highest stability at 650K due to the lower Au diffusion rate in Ti than in other systems and due to the fact that the Ni₂Si phase forming in the Ni layer starts playing the role of a

diffusion barrier and prevents Au diffusion toward the substrate. The experiments confirm the multistage character of mass transfer in thin-film Ti-Ni-Au, W-Ni-Au, and Mo-Ni-Au systems. Figures 2; tables 4; references 2.

Optimizing the Composition of Deposited Metal and Parameters of Wear-Resistant Buildup Techniques

937D0034C Moscow SVAROCHNOYE
PROIZVODSTVO in Russian No 8, Aug 92 p 19

[Article by L. S. Livshits, Doctor of Technical Sciences, and O. Yu. Yelagina, engineer, State Academy of Oil and Gas im. I. M. Gubkin; UDC 621.791.927.93]

[Abstract] A computer program was developed for calculating conditions of buildup of worn parts by the manual arc method and the structure of the deposited metal for the purpose of optimizing the conditions according to wear-resistance criteria. Controllable input parameters of buildup conditions included the current and voltage of the arc, rate of buildup, and heating of the part, and uncontrollable parameters included ambient temperature, thickness of the part, and chemical composition and thermophysical properties of the primary and electrode metals. For the calculated values a set of factors was established which affect the stability of the process and the quality of the deposited layer: critical length of the arc, incomplete fusion of the primary metal, maximum permissible pressure of the arc on fused metal, and maximum permissible heating of the electrode by the passing current.

It was found that analysis of values of buildup process parameters permits selection of conditions for obtaining the required dimensions of the bead and the fusion zone. Changing buildup conditions results in a substantial change in the structural-phase state of the deposited metal, and consequently its wear resistance. Given the availability of a variety of materials for building-up, it is possible to select not only buildup conditions but also a chemical composition of deposit metal which ensures the highest hardness.

Laser Technology for Imparting Tribotechnical Characteristics to Friction Surfaces

937D0034E Moscow SVAROCHNOYE
PROIZVODSTVO in Russian No 8, Aug 92 pp 22-25

[Article by V. S. Avanesov, Candidate of Technical Sciences, State Academy of Oil and Gas im. I. M. Gubkin; UDC 621.791.947.72:621.375.826]

[Abstract] Causes of parasitic perturbations in laser forming of the microrelief of friction surfaces using melting and some ways of suppressing them to reduce allowances were investigated. Phenomenological models of the formation of periodic surface structures (pronounced periodicity in a wavy relief) make it possible to discern some approaches to suppressing parasitic perturbations.

A model experiment was used to investigate the kinetics of fusion of micro-unevennesses on surfaces. Conical specimens with different tip angles were melted with a CO₂ laser with 0.9 kW power and a focal spot diameter of 4 mm. The possibility of using a laser to improve surface microrelief (laser "polishing") was demonstrated.

The possibility of laser etching of friction surfaces to create a system of depressions that form a regular relief for lubricants was also demonstrated. These "oil channels" increase the stability of the lubricant film that forms and facilitate the removal of products of wear from the friction zone.

Modification of the Surface Layer of Parts by Micro-Arc Oxidation

937D0034G Moscow SVAROCHNOYE
PROIZVODSTVO in Russian No 8, Aug 92 pp 29-30

[Article by V. A. Fedorov, Candidate of Technical Sciences, State Academy of Oil and Gas im. I. M. Gubkin; UDC 621.794.61:621.357.8:669.715]

[Abstract] Results of investigation of surface layers of aluminum alloys hardened by the micro-arc oxidation process are presented. The alloys were categorized into four groups according to mechanical properties, chemical composition and other parameters, and specimens of specific brands of alloys from each group were treated using three different modes of micro-arc oxidation. The composition and structure of the resulting hardened layers were examined by x-ray diffraction. It was found that in most of the alloys the hardened layer has a crystalline structure, unlike anode oxide films formed by conventional anodizing. The phase composition of the hardened layer depends on the micro-arc oxidation mode, the layer thickness, and the chemical composition of the oxidized material. Oxide phases were not found to have a pronounced grain orientation, indicating a random orientation of crystals in the hardened layer. Results of studies of micromechanical properties, crack formation, and tribotechnical characteristics of hardened layers are also presented.

Wear Resistance of Coatings Based on Metalide Alloys

937D0034H Moscow SVAROCHNOYE
PROIZVODSTVO in Russian No 8, Aug 92 pp 33-34

[Article by V. A. Neuymin, S. A. Shelukha, G. A. Leontyeva, and Ye. N. Tarasenko, Norilsk Mining and Metallurgical Combine; UDC 621.791.052:539.538]

[Abstract] Results of investigation of the main characteristics of different metalide coatings under conditions of abrasive wear and how these characteristics differ depending on spray-coating conditions are presented. Coatings were applied using the plasma spraying unit WSP 1500/500. Materials for spray coating were the

metalide alloys PN85Yu15 (Ni-Al system) with a 160-micrometer fraction, and PN55T45 (Ni-Ti) with 10-45 and 40-100-micrometer fractions. Test results showed that relative wear of metalide coatings of the Ni-Ti system (PN55T45) is on average 3.2 times lower than that of coatings of the Ni-Al system (PN85Yu15). The best characteristics in conditions of abrasive wear belong to the coating PN55T45 using a powder fraction of 10-45 micrometers and a sublayer of the Ni-Cr alloy Kh20N80. It was also found that in spraying coatings of the Ni-Ti system, additions of hydrogen in the plasma jet can lead to increased pore formation and cracking of the coating, which is due to increased enthalpy of the plasma flow.

Structure and Properties of Coatings Applied with a CO₂ Laser

927D0225D Moscow METALLOVEDENIYE I
TERMICHESKAYA OBRABOTKA METALLOV
in Russian No 7, Jul 92 pp 18-21

[Article by V. Ye. Arkhipov, A. A. Ablayev, and L. T. Krasnov, All-Union Scientific and Production Association "Remdetal"; UDC 621.9.048.7:621.762]

[Abstract] The structure and properties of 45 coatings applied to steel with a CO₂ laser were investigated. The coating materials used were self-fluxing nickel-base powders containing different amounts of carbide and boride forming elements. Different effects on the structure and properties of coatings were determined for different compositions of powder materials and different parameters of their application with the laser. Treated specimens were examined using the methods of metallographic analysis and luminescence analysis. The analyses produced the following conclusions:

1. Decreasing the chromium and carbon contents in the powder material of the system Ni-Cr-B-Si makes the coating less likely to crack.
2. Preheating the substrate specimen to 100-150 degrees C almost completely eliminates the tendency of the coating to crack when nickel-base self-fluxing powders are used as the coating material.
3. The corrosion resistance of coatings applied with the laser is as high as that of chrome-plating, and such coatings have a long service life even when cracks do form on the surface.
4. Coatings are highly resistant to scoring both at room temperature and higher temperatures, and their resistance to wear is an order of magnitude greater than the wear resistance of steel 45 which has been heat treated to a hardness of 51-53 HRC.

Corrosion Resistance of Tubular Parts Coated With Z-Al Alloy

937D0097D Moscow ZASHCHITA METALLOV
in Russian Vol 29 No 1, Jan-Feb 93 (manuscript
received 28 Aug 91) pp 111-114

[Article by Ye.V. Proskurkin, I.Ye. Mitnikov, A.I. Sukhomlin, S.V. Zekhov, and A.Yu. Norvillo, All-Russian State Scientific Research and Manufacturing Institute of Pipe Institute, Dnepropetrovsk; UDC 541.138.3:620.193.01]

[Abstract] Branch pipes made of B-St2 or B-St3 plain carbon steel with two different protective Zn-Al alloy coatings, "Galfan" alloy (93.71-95.25% Zn, 4.7-6.2% Al, 0.02-0.05% Ce, 0.03-0.04% La) and "Galvanium" alloy (43.4% Zn, 55.0% Al, 1.6% Si), were tested for corrosion resistance in 3% aqueous NaCl solution at room temperature, in industrial coke oven gas during scrubbing with monoethanolamine, and in a hot water supply plant. All branch pipes were 75 mm long, but were of four different sizes (outside diameter and wall thickness: (1) 20.3 mm and 2.5 mm, (2) 26.3 mm and 2.5 mm, (3) 33.5 mm and 2.8 mm, (4) 42 mm and 2.8 mm). All pipes were degreased, washed, etched, and rinsed prior to three different treatments: (1) with aqueous solution of flux containing chlorides of metals and a wetting agent, followed by drying at 200 +/- 10°C; (2) with solution containing chromium anhydride for formation of passive film, followed by drying in warm (70 +/- 10°C) air stream; (3) with zinc melt at 460°C for 10-15 s for formation of thin passive zinc layer. They were then coated by dipping for 20-40 s in the alloy melt at 480 +/- 10°C ("Galfan") and at 620 +/- 10°C ("Galvanium"), for 20-180 s at 780 +/- 10°C after treatment with passivating solution. Coating was done in a 2.5 kW electric shaft furnace with a 300 mm high and 120 mm diameter heating zone. Subsequent cooling of the coated pipes was done either quickly by quenching in water or slowly by soaking in air. The corrosion tests in 3% aqueous NaCl solution were accelerated by cycling "10 min in solution - 30 min in air" for a total of only 625 h. The corrosion tests in coke oven gas were conducted regularly for 3968 h. The corrosion tests in Dnepropetrovsk hot water supply plants were conducted with the branch pipes in the bypass and with hot water (55-60°C) for customers flowing through the feed line at a velocity of 0.5 m/s under a pressure of 6 atm. The results indicate that in both NaCl solution and coke oven gas, "Galvanium" coatings and especially those on a zinc sublayer are much more corrosion-resistant than conventional hot-dip zinc coatings and "Galfan" coatings on an oxide sublayer. In a hot water supply plant, "Galvanium" coatings on a zinc sublayer were, after 7225 hours, found to have corroded at a rate of only 19 µm/yr, conventional hot-dip zinc coatings having corroded at a rate of 34 µm/yr and bare steel pipes having corroded at a rate of 292 µm/yr. The authors acknowledge participation of A.A. Verbitskaya, V.P. Vlasova, and N.N. Sidorova in this study. Figures 2; reference 5.

Electrolyte for Deposition of Ni-Teflon Composite Coatings

937D0097E Moscow ZASHCHITA METALLOV
in Russian Vol 29 No 1, Jan-Feb 93 (manuscript
received 9 Jul 90) pp 160-162

[Article by N.M. Teterina and G.V. Khaldeyev, Perm State University imeni A.M. Gorkiy; UDC 621.357:669.018.95]

[Abstract] Since formation of a stable and uniform composite, electrochemical coatings of the Ni-PTFE (polytetrafluoroethylene) kind from Watt's electrolyte is difficult because PTFE is hydrophobic, three electrolytes contain nickel acetate or both nickel sulfate and boric acid in addition to nickel chloride: A. 180 g/l $\text{Ni}(\text{CH}_3\text{COO})_2 \times 4\text{H}_2\text{O} + 30 \text{ g/l NiCl}_2 \times 6\text{H}_2\text{O}$ (pH 4.2, T = 20°C), B. 300 g/l $\text{Ni}(\text{NH}_2\text{SO}_3)_2 \times 4\text{H}_2\text{O} + 15 \text{ g/l NiCl}_2 \times 6\text{H}_2\text{O} + 35 \text{ g/l H}_3\text{BO}_3$ (pH 3.6, T = 20-40°C), C. 200 g/l $\text{Ni}(\text{NH}_2\text{SO}_3)_2 \times 4\text{H}_2\text{O} + 15 \text{ g/l NiCl}_2 \times 6\text{H}_2\text{O} + 35 \text{ g/l H}_3\text{BO}_3$ (pH 3.8, T = 20-40°C). The nonionogenic surfactant "Neonol-9" was added in concentrations of 0.5 g/l and 1 g/l, to each electrolyte for stabilization of PTFE particles in the suspension, the stability limits being determined on the basis of optical density measurements in a KF-77 photocalorimeter through an optical filter for 535 nm light. Electrostatic repulsion forces were found to be negligible and chemisorptive interactions to be sufficiently strong. Relative concentrations $[\text{Ni}(\text{CH}_3\text{COO})^+]$ ions and $[\text{Ni}(\text{CH}_3\text{COO})_2]$ molecules in electrolyte A were calculated by numerically solving the system of five equations on an "Iskra 1030" computer: two equations of material balance and three equations representing the law of acting masses. The optimum conditions for depositing Ni-PTFE coatings from this electrolyte were thus found to be pH 5 and T = 20°C. Figures 2; tables 2; references 3.

Approximate Design of Potential Transducers for Inspecting Electrochemical Protection of Underground Steel Pipes

937D0097B Moscow ZASHCHITA METALLOV
in Russian Vol 29 No 1, Jan-Feb 93 (manuscript
received 14 Jan 92) pp 29-35

[Article by L.I. Freyman, Academy of Municipal Economy; UDC 620.197.5]

[Abstract] The potentiometric method of inspecting cathodic protective coatings on underground steel pipes with the aid of polarization potential transducers is considered, obtaining approximate formulas for design analysis and optimization of the transducer electrodes. A through defect such as a hole in the protective coating is schematically drawn as a frustum of a regular pyramid with the smaller base on the steel surface, the larger base on the outer coating surface, and all lateral walls sloping at the same angle. A frustum of a regular square pyramid is selected, this being the simplest geometrical model for calculations, and the wall sloping angle is varied from 40° to 90°. The design calculations are based on an

equation that relates the ohmic electrode-soil contact resistance to the resistance of the soil and the diffusion resistance at the channel inlet. These resistances are related through three parameters in the equation: two characteristic numbers representing properties of the soil and one dimensional parameter, the "effective electrode length," this parameter depending only on the shape and size of the electrode and on the thickness of the coating. The exposed steel surface is assumed to be an equiaxial active one. A numerical design analysis for plane triangular, hexagonal, square, and rectangular electrodes demonstrates that this model adequately covers all kinds of through defects in the coating for optimum transducer selection in any specific case. Figures 1; tables 3; references 18.

Atmospheric Corrosion of Metals and Alloys in "Mirnyy" Station in Antarctica

937D0097A Moscow ZASHCHITA METALLOV
in Russian Vol 29 No 1, Jan-Feb 93 (manuscript
received 2 Mar 92) pp 12-19

[Article by A.A. Mikhaylov, Yu.N. Mikhaylovskiy, N.F. Sharonova, M.N. Suloyeva, A.M. Soshnikov, V.M. Loginov, A.V. Parfenov, and A.A. Kotov, Institute of Physical Chemistry at Russian Academy of Sciences, Institute of Arctic and Antarctic Regions at USSR State Committee on Hydrometeorology; UDC 620.193.2]

[Abstract] Following a comprehensive description of Antarctica's climate based on numerous data collected at the various research stations (Adelaide Island and Bellingshausen in the moderate region with moderate winds, "Mirnyy" and "Molodezhnaya" in the moderate region with strong winds, "Halley" and "Scott's Hat" near Scott Base in the cold region with moderate winds, "Pionerskaya" and "Mitsuho" in the cold region with strong winds), a report is given on atmospheric corrosion tests performed from 9 May 1989 to 16 April 1990 at the "Mirnyy" station (USSR). The tests were performed on 100x150 mm² bars of St-3 plain carbon steel (0.15% C, 0.42% Mn, 0.024% P, 0.013% S, traces of Si), 99% pure copper, 99.7% pure cadmium (0.02% P, 0.13% Cu, 0.003% Zn, traces of Fe), and D-16 aluminum alloy (92% Al, 1.2-1.8% Mg, 0.38-0.49% Cu, 0.3-0.9% Mn, 0.3

Zn, less than 0.5% Si, less than 0.5% Fe), the principal corroding agent in the air being chlorine ions. For shipment to Antarctica, after appropriate treatment, they had been kept in polyethylene bags containing volatile corrosion inhibitors. There they were taken out and mounted in special cassettes for testing, each cassette holding six bars of only one material. The test stand was oriented in the south-north direction, with the cassettes inclined at a 45° angle. In the first month (May 1989) the temperature ranged from -29.1°C to -7.0°C, the relative humidity ranged from 52% to 98%, and the average velocity of winds blowing predominantly eastward was 11.8 m/s. In the coldest month (July 1989) the temperature ranged from -30.7°C to -5.4°C, the relative humidity ranged from 48% to 98%, and the average

velocity of winds blowing predominantly in the SSE direction was 13.2 m/s. In the warmest month (December 1989) the temperature ranged from -8.5°C to +3.6°C, the relative humidity ranged from 41% to 100%, and the average velocity of winds blowing predominantly eastward was 11.3 m/s. In the last month (April 1990) the temperature ranged from -20.4°C to -5.9°C, the relative humidity ranged from 53% to 94%, and the average velocity of winds blowing predominantly in the SE direction was 14.0 m/s. The corrosion rate was measured in terms of yearly weight loss (g/m²/yr) and yearly scale buildup (μm/yr). The results indicate that the corrosion rates of these four materials in Antarctica are comparable with their corrosion rates measured earlier in corresponding Arctic regions (Ayon Island, Apapellhino Peninsula, Cape Schmidt). They also indicate that precipitation of aerosols of chlorides ascending from the ocean causes fast corrosion of these materials at temperatures below -1°C. Figures 1; tables 6; references 15.

Estimating Corrosion Resistance of Welded Ti-Alloy Joints by Polarization Resistance Method

937D0097C Moscow ZASHCHITA METALLOV
in Russian Vol 29 No 1, Jan-Feb 93 (manuscript
received 29 Mar 88) pp 55-63

[Article by S.G. Polyakov, G.M. Grigorenko, V.N. Zamkov, G.Ye. Boyeva, and A.G. Fedorenko, Institute of Electric Welding imeni Ye.O. Paton at Ukrainian Academy of Sciences; UDC 620.193.01]

[Abstract] The polarization resistance method of estimating the corrosion resistance was experimentally applied to welded Ti-alloy joints, WTi1-0 and PTi-3V joints, which were selected for this test. Electric welding was done in an automatic machine with a current of 450 A at 11-12 V, 150 mm long 3x30mm² wide at a rate of 5 mm/s without separation of edges and addition of a filler. The joints were heat treated at 1020°C either in air or under vacuum, whereupon specimens containing a 3x10x30 mm³ large volume of parent material, a 3x6x30 mm³ large seam segment, and a 3x3x30 mm³ large adjacent segment of the heat-affected zone were cut out for testing. After a current lead of titanium wire 2 mm in diameter had been welded to each strip, the surface of each strip was first thoroughly cleaned with successively finer emery papers and glass powder, then degreased with acetone and ethanol, rinsed with warm distilled water, air-dried, and finally weighed. As the corroding medium was selected as 5% aqueous H₂SO₄ solution, its temperature was maintained at 50°C. Two identical weld specimens were placed 20 mm apart in a glass cell with an inversion cooler, one of which was connected to an AgCl reference electrode through a Luggin capillary probe. The polarization resistance was measured by the potentiostatic method with a UISK-2 corrosimeter using two electrodes, the polarization curves being plotted with a P-5827 potentiometer and a V7-21 high-resistance voltmeter. Both corrosion potential and polarization resistance were also independently measured. According to this method of measurement,

the corrosion rate is proportional to the ratio of current increment ΔI to overvoltage ΔE (10 mV) with a proportionality constant B that depends on the loss of weight and is inversely proportional to the active surface area. This method thus facilitates determination of instantaneous corrosion rates with minimum distortion of the system. The evaluation of the test data is most expediently based on an equivalent circuit that simulates the metal-electrolyte interface so as to take into account dissolution of the metal but, for simplicity, ignores diffusion processes. The results indicate that the method is applicable to welded Ti-alloy joints, with the constant $B = 43 \pm 5.7$ mV. Figures 4; tables 3; references 9.

The Effect of Molybdenum Content on Intercrystalline Corrosion in KhN40MDB Alloy

937D0098A Moscow ZASHCHITA METALLOV
in Russian Vol 29, No 2, Mar-Apr 1993 pp 231-234

[Article by E. T. Shapovalov and M. Yu. Ustimenko;
UDC 620.193.23:669.14]

[Abstract] Several alloys made of 20% Cr, 40% Ni, and 30% Fe, in which the Mo content varied from 0 to 7.7%, were studied to determine their susceptibility to intercrystalline corrosion. The alloys were heat-treated in three ways: (1) quenching from 1080°C in water for 25 min.; (2) same quenching procedure, plus annealing at 700°C for one hour; and (3) same quenching procedure, plus annealing at 700°C for 10 hours. Polished specimens were tested for intercrystalline corrosion using weakly oxidizing (corrosion potential +0.35 V, 24 and 120 hour test periods; +0.35 V, 8 and 24 hours), and strongly oxidizing (GOST 6032-89) (+0.85 V, 48 and 96 hours) weight-loss coupon testing methods. The specimens were also exposed to a boiling 20% solution of HCl for five hours. It was found that all the specimens were resistant to intercrystalline corrosion, which was observed only in

the Mo-alloyed tempered specimens, even after the prolonged testing periods. The alloy's resistance to intercrystalline corrosion is determined by the electrochemical corrosion properties of the molybdenum, which converts to a transpassive state at a potential of +0.4 V and induces the proeutectics, of which it is a component, to do the same. Under weakly oxidizing conditions, an increase in Mo content promotes increased corrosion resistance, but has the opposite effect under strongly oxidizing conditions, primarily due to the selective dissolution of the Mo-containing phases that precipitate out along the grain boundaries. In the reducing medium, Mo alloying noticeably reduces total loss of mass, but imparts a caustic nature to the corrosion along the grain boundaries where the solid solution is relatively poor in molybdenum. Figures 1, tables 2; references 7; 5 Russian, 2 Western.

Durability of Corrosion-Resistance Polymer Coatings for the External Surfaces of Underground Pipelines

937D0098B Moscow ZASHCHITA METALLOV
in Russian Vol 29, No 2, Mar-Apr 1993 pp 297-300

[Article by Yu. I. Garber; UDC 620.197.6:621.643.2/3]

[Abstract] The main causes of damage to the low-density polyethylene films used to coat underground oil-and-gas pipelines in Siberia and the Far North were summarized. The coatings, which are applied in the field by insulating machines, are subjected to extreme tensile stresses brought about by creep in the coatings' adhesives, the action of soil characteristics such as the presence of surfactants and moisture, the mechanical properties of the soil, the weight of the pipes themselves, friction between the pipe and the trench bed and sides, and so forth. These stresses result in various types of obvious defects in the coatings, including perforations, tears, cracks, wrinkles, etc., that adversely affect coating durability. Figures 4, references 3; Russian.

Behavior Characteristics of Physical Properties of VNL Steels in Liquid State

937D0112A Moscow METALLY in Russian No 3.
May-Jun 93 pp 13-16

[Article by L.A. Oborin, Ye.Ye. Tretyakova, B.A. Baum, A.I. Cherepanov, V.V. Vyukhin, G.V. Tyagunov, E.V. Kolotukhin, M.V. Rovbo, V.S. Tsepelev, Yekaterinburg; UDC 669.15-194.3]

[Abstract] The physical properties of VNL1, VNL2, and VNL6 steels are investigated and their chemical composition is summarized. In particular, the kinematic viscosity, surface tension, electric resistivity, and critical temperatures of the steels are examined by studying the polythermal curves of the physical properties. The polythermal curves of kinematic viscosity and surface tension of liquid VNL steels under heating and cooling are plotted. The steels display a similarity of properties with respect to the principal alloying constituents, i.e., Cr and Ni, and the C, Si, and Mn concentration but differ in the behavior of the Mo, Cu, Nb, and Co concentration. All polythermal curves are characterized by hysteretic properties, i.e., a spread between the cooling and heating branches. The effect of the chemical composition and solid metal structure on the magnitude and shape of these curves is discussed. An analysis demonstrates that an increase in the degree of melt equilibrium before solidification primarily facilitates a more uniform austenite distribution in the martensitic structure. This, in turn, attests to a more uniform distribution of elements before solidification and helps reduce the number of structure defects, including those of the shrinkage origin, which is probably due to a change in the melt structure and thermal parameters, a decrease in the segregation temperature, and a change in the casting characteristics of liquid steel. Figures 2; tables 2; references 2.

Structurization of Grain-Oriented Electric Steel During Annealing in Various Atmospheres

937D0107C Moscow STAL in Russian
No 1, Jan 93 pp 76-77

[Article by A.G. Dukhnov, A.M. Chernykh, V.P. Baryatinskiy, and S.I. Plotnikov, Central Scientific Research Institute of Ferrous Metallurgy, Lipetsk branch; UDC 669.14.018.583]

[Abstract] An experimental study of grain-oriented, cold-rolled electrical steel alloyed with about 0.5% Cu + 0.20% Mn and also containing 0.010-0.016% Al was made, the object being to examine its behavior during high-temperature annealing in various controlled atmospheres. After decarburization, 0.75 mm thick stock was cold-rolled to 0.21 mm, 0.23 mm, 0.25 mm, and 0.27 mm thick sheets. The sheets were cut into three batches of 610 mm long strips for annealing in three different atmospheres:

(1) electrolytic hydrogen

(2) protective nitrogen (99% N₂ + 1% H₂)

(3) argon

Each atmosphere, in a tubular furnace, contained 0.0005% O₂ and less than 0.001% moisture. Preliminary gradiental annealing for 1 h, one end of a strip having been heated to 1100°C at a rate of 30 K/h and the other end having been heated to 300°C, was followed by final high-temperature annealing at 1150° for 5 h in the same atmosphere. The results of macro- and microstructural examination after each annealing treatment reveal a strong dependence of the primary recrystallization process on the atmosphere in which the preliminary gradiental annealing had taken place. The temperature interval of primary recrystallization was found to be 470-585°C in a hydrogen atmosphere, 530-585°C in a protective nitrogen atmosphere, 450-530°C in an argon atmosphere. Maximum grain growth, up to a 42 µm size fraction, with maximum consertality had occurred in argon. Secondary recrystallization and attendant grain texturization were in each case completed at 900°C, both processes depending on the oxidation-reduction processes at the steel surface. The results of grain orientation analysis and magnetic tests indicate which atmosphere is most favorable for each thickness of cold-rolled electrical sheet steel: hydrogen for 0.27 mm thick sheet, protective nitrogen for 0.23 mm and 0.21 mm thick sheet. All three atmospheres are almost equally favorable for annealing sheet of the 0.25 mm intermediate thickness. Tables 2.

Continuous Casting of 12Cr18Ni10Ti Steel in Horizontal MNLZ Casting Machine with Bilateral Extraction of Ingot without Scarfing of Cast Metal

937D0107A Moscow STAL in Russian
No 1, Jan 93 pp 37-38

[Article by A.M. Chigrinov, V.M. Parshin, I.I. Sheynfeld, L.P. Zakov, M.F. Panin, and M.D. Zharnitskiy, Central Scientific Research Institute of Ferrous Metallurgy, Scientific-Industrial Association: All-Union Scientific Research, Planning, and Design Institute of Metallurgical Machinery, "Hammer and Sickle" Metallurgical Production Plant; UDC 669.14.018.8:621.746.047]

[Abstract] A new technology has been developed for casting 12Cr18Ni10Ti corrosion-resistant steel in a horizontal MNLZ (Continuous Ingot Casting) machine, namely bilateral extraction of an ingot without its subsequent scarfing. The casting machine is 6 m wide, 2.2 m tall, and 25 m long. The molten metal flows from a hopper down through a vertical tube into a crystallizer that has a 140 mm square cross-section and is cast here at a rate that can be varied over the 0.7-1.2 m/min range. The liquid metal flows downward from the furnace through a vertical conduit into a crystallizer, the entire system being enclosed and designed so that nonmetallic inclusions, as well as air bubbles, rise to the surface rather than fall into the crystallizer. Ingots of practically

pure steel are then extracted from the crystallizer horizontally through two lateral orifices on opposite sides. The vertical tube, with an inside diameter not larger than 0.5 mm, is made preferably of a refractory material with a melting point above 1750°C and the temperature at both crystallizer orifices should be above 1480°C. Since casting 12Cr18Ni10Ti steel requires stringent temperature-rate regulation, the reciprocating crystallizer motion and the rocking furnace motion are tuned to a frequency that precludes transverse cracking of ingots. Maintenance of a constant ferrostatic pressure in the crystallizers and thus stabilization of the casting process are ensured by appropriate dimensions of both crystallizer orifices within the 20-100 mm diameter range. The temperature of an ingot leaving the crystallizer for extrusion at a constant rate is within the 1100-1200°C range, its shape being determined by conditions inside the crystallizer. Secondary cooling by spraying is adequate with either 0.2 or 0.3-0.5 liter of water per kilogram of steel. The temperature of ingots leaving the MNLZ machine after extrusion is about 750°C, which allows direct transfer of 1.4-1.6 m long ingots 120-175 mm square in cross-section to a rolling mill without their prior "hot dip" scarfing. The machine is designed for casting 15-30 tons of steel per hour, its annual output being 5% higher than that of a vertical or radial continuous casting machine. It weighs 60 tons, not including the shears. The authors acknowledge participation of Z.N. Fedorov (Central Scientific Research Institute of Ferrous Metallurgy), V.M. Shukin and V.A. Reshetov (All-Union Scientific Research, Planning, and Design Institute of Metallurgical Machinery), A.F. Kolosov, G.P. Patrikeyev, and L.M. Lastovetskiy ("Hammer and Sickle" Metallurgical Production Plant) in the project. Figures 2.

Structural and Technological Prerequisites for Producing New Generation of Grain-Oriented Electrical Sheet Steel

937D0107B Moscow *STAL* in Russian No 1.
Jan 93 pp 74-76

[Article by G.A. Brashevan, M.M. Borodkina, L.M. Krylova, F.M. Golyayeva, and V.P. Vladimirov, Central Scientific Research Institute of Ferrous Metallurgy; UDC 669.14.018.583]

[Abstract] An experimental study of grain structuring in high- μ m electrical sheet steel (0.04-0.05% C, 22.9-3.05% Si, 0.07-0.09% Mn, 0.035% Al, 0.024-0.028% S, 0.006% N) was made, its grain orientation depending on the fabrication process and on the state of corrosion-inhibiting phases. Steel ingots produced by the Chelyabinsk Metallurgical Combine were hot-rolled down to 2.5

mm thick sheets, the initial and final rolling temperatures being 1350-1320°C and 980-1000°C respectively. These sheets were normalized according to two different schemes:

(1) heating from about 500°C to 1100°C followed by stepwise air cooling to 1040°C \rightarrow 870°C and then air+water cooling to 580°C \rightarrow 350°C \rightarrow 100°C, total cooling time about 4 min

(2) heating to 1150°C followed by stepwise air cooling to 1080°C \rightarrow 900°C and then air+water cooling to 580°C, total cooling time about 3 min, followed by slow cooling to 100°C. After normalization they were cold-rolled to 0.30 mm, 0.23 mm, and 0.18 mm thicknesses. Sheets that had been normalized according to the first scheme were cold-rolled as follows:

(1) three batches in one draw to 0.30 mm, 0.23 mm, and 0.18 mm, respectively

(2) one batch in two draws to 0.7 mm \rightarrow 0.23 mm and one batch in two draws to 1.2 mm \rightarrow 0.18 mm

(3) one batch in three draws to 1.2 mm \rightarrow 0.5 mm \rightarrow 0.18 mm, with recrystallizing heat treatment at 860°C for 10 min between second and third draws. Sheets that had been normalized according to the second scheme were cold-rolled as follows:

(1) one batch in one draw to 0.23 mm

(2) one batch in two draws to 0.7 mm \rightarrow 0.23 mm and one batch in two draws to 1.2 mm \rightarrow 0.18 mm.

All sheets were subsequently decarburized by preliminary heat treatment at 820°C or 900°C in a nitrogen+hydrogen atmosphere for 10 min and final high-temperature heat treatment at 1180°C in a pure hydrogen atmosphere, the heating rate having been regulated to that high temperature according to standard procedure. Structural examination and phase analysis revealed maximum predominance of the favorable [curly bracket] 111 [curly bracket] grain orientation in sheets rolled down to 0.18 mm in one draw. Cold rolling to 0.23 mm in one draw had improved the magnetic properties, combining high magnetic induction and low core loss, without appreciably changing the concentration and distribution of inhibitors. The concentration of inhibitors in 0.18 mm thick sheets must be maintained at 10^{14} cm $^{-3}$ or even raised to 10^{15} cm $^{-3}$ prior to secondary recrystallization, if detrimental effects not only on grain orientation and corrosion inhibition, but also on magnetic properties are to be prevented. This is achieved by injection of a nitrogen compound into the coating (MgO) so that nitrogen will then diffuse into the base metal. Figures 3; tables 1; references 2.

Electrical Steels with High Silicon Content

937D0107D Moscow *STAL in Russian* No 1,
Jan 93 pp 81-82

[Article by A.P. Khomskiy, Central Scientific Research
Institute of Ferrous Metallurgy; UDC 669.14.018.583]

[Abstract] New are methods available for producing cold-rolled electrical steels with a higher than 3.2% Si content and with not only excellent magnetic properties, but also adequate plasticity. Embrittlement, caused by solid-solution hardening and more so by atomic ordering, is now avoided by deep vacuum refining for removal of detrimental impurities (C,S,P,N₂) and by addition of grain-crushing modifiers so that more silicon can be added without penalty. Chemically saturating the steel with silicon is not expedient because the steel becomes brittle due to the formation of silicide during high-temperature treatment and slow subsequent slow cooling.

Neither does fast cooling of the melt at rates up to 10^3 K/s facilitate cold rolling of even only 0.1-0.2 mm thick cast and quenched ribbon containing more than 5.2% Si. An effective method for steels with up to 6.5% Si is to precede cold rolling with an initial hot draw followed by an intermediate warm draw at a temperature within the range of intense atomic ordering, the purpose of such a draw being to suppress this ordering process and thus increase the plasticity sufficiently to attain at least 75% total reduction by this draw. Another effective method is surface treatment with a laser ensuring extremely high local heating and cooling rates of 10^3 - 10^4 K/s, which will suppress atomic ordering in up to 500 μ m thick surface layers on both sides of a sheet. Magnetic core laminations are considered 5.0% Si steel punchable after high-temperature treatment in lieu of 6.5% Si steel punchable only after cold rolling, the specific power loss (W/kg) in a core of 5.0% Si steel being not more than 10% higher than in a core of 6.5% Si steel. Tables 1; references 5.

Resource Conservation and Improvement of Nickel-Based Superalloy Casting Performance by High-Temperature Melt Treatment

937D0106A Moscow METALLY in Russian No 1, Jan-Feb 93 pp 31-37

[Article by B.A. Baum, V.N. Larionov, L.V. Kovalenko, G.V. Tyagunov, Ye.A. Kuleshova, Ye.Ye. Baryshev, Ye.Ye. Tretyakova, E.V. Kolotukhin, Sverdlovsk; UDC 54.14:669.245:669.046]

[Abstract] The under-utilization of production conditions brought about by the chemical composition of cast parts from Ni-based superalloys due to the high number of cast metal defects, especially in gas turbine engine parts, prompted a study of the possibility to conserve resources and improve the performance of castings by high-temperature melt treatment (VTOR). The stages involved in developing the high-temperature melt treatment conditions are outlined in detail; the polythermal curves of the superalloy's resistivity during heating and cooling, the temperature dependence of kinematic viscosity, surface tension, and density of molten superalloys during heating and cooling, the effect of the maximum heating temperature of molten superalloys on the structural factor type, and the dependence of the superalloy supercooling on superheating are plotted. The study reveals the relationship between the temperature-time parameters of the melt preparation process and the solid alloy structure and properties and makes it possible to develop resource conserving high-temperature melt heat treatment practices that improve the metal quality and performance, reduce the number of rejects, and help save highly scarce materials. In addition, the method makes it possible further to increase the alloy's high-temperature strength by 10-30°C. Figures 5; references 4.

Mixing Volume Correlation of Binary and Ternary Ni-Fe-Mo Alloys

937D0106B Moscow METALLY in Russian No 1, Jan-Feb 93 pp 49-52

[Article by V.V. Leonov, G.A. Nikiforov, Ye.Yu. Belmash, Krasnoyarsk; UDC 669.245:541.1]

[Abstract] The importance of mixing volume for understanding the thermodynamics of solutions prompted an attempt to demonstrate that one can determine the total volume and mixing volume of a ternary metallic alloy if one knows the alloy composition and total mixing volumes of the binary alloys forming it. The experimental procedure involving 54 ternary and 22 binary metal single-phase Ni-Fe-Mo alloys studied with a DRON-3 diffractometer using known methods is described. The dependence of the single mole volumes of Ni-Fe-Mo single-phase ternary alloys on the mole fraction ratios at

a constant nickel concentration in various alloys and the dependence of the mixing volumes of a single mole of single-phase ternary Ni-Fe-Mo alloys on the mole fraction ratios at a constant Ni concentration in various alloys are plotted. The findings confirm the possibility of calculating the mole and mixing volumes of single-phase ternary alloys using data obtained for the corresponding binary alloys. A check demonstrates that the deviation of the experimental data on total volumes from the results obtained by analytical formulae is small enough, thus attesting to the validity of some of the formulae derived in the study. Figures 2; references 3.

On Issue of Dendritic Inhomogeneity in Single Crystal Ingots From YuNDKT5AA Alloy Grown at Various Rates

937D0106C Moscow METALLY in Russian No 1, Jan-Feb 93 pp 94-97

[Article by I.V. Belyayev, M.V. Pikunov, A.A. Vostryakov, L.I. Baranov, Moscow; UDC 548.55:669.018.58:620.192.3-172]

[Abstract] The nonmonotonic behavior of the coefficient of dendritic segregation of elements with an increase in the growth rate of single crystals of the YuNDKT5AA magnetically hard alloy is discussed and an attempt is made to find the reason for the nonmonotonic dependence of dendritic segregation on the growth rate; to this end, the cooling rates are measured at various points of YuNDKT5AA alloy ingots being grown by thermocouples, and the resulting data are compared to the value of dendritic segregation. The dependence of the segregation coefficient of Ti and Al on the YuNDKT5AA alloy cooling rate within the crystallization range, the Ti and Al concentration behavior at the center of dendritic cells in the YuNDKT5AA alloy with an increase in the cooling rate within the crystallization range, and the behavior of the final solidification temperature of the YuNDKT5AA alloy with an increase in the cooling range within the crystallization range are plotted. The findings obtained by a Camebax X-ray microanalyzer show that given cooling rates used for growing single crystals from the YuNDKT5AA alloy, the chemical composition of the central part of dendritic cells does not remain constant while the extreme values of all plots fall within the same range of cooling rates. It is speculated that as the cooling rate increases, the liquid phase composition of the crystallizing alloy may change so much that we are actually dealing with another alloy with its own final crystallization temperature and element distribution coefficients whereby each cooling rate seems to correspond to a new alloy composition. The non-monotonic behavior of dendritic segregation with an increase in the cooling rate is attributed to the latter phenomenon. Figures 3; references 7.

On Martensitic Transformations in Fe- and U-Based Alloys

937D0106D Moscow *METALLY in Russian No 1*, Jan-Feb 93 pp 112-116

[Article by A.N. Kobylkin, A.G. Nikolayev, V.G. Koshe-lyayeva, M.Ya. Eydinov, Moscow; UDC 620.181.4:669.112.2]

[Abstract] This article discusses metastable constitution diagrams of metal systems and the problems with developing equipment for plotting polythermal cross sections at high cooling rates (from the annealing to the hardening temperature), which are divided according to both the high cooling rates and the methods of recording and processing thermocouple signals. Methods of carrying out a high-speed thermal analysis of the phase transformations, particularly martensitic transformations, at cooling rates of up to 1,000°C/s within a 1,000-800°C rate are outlined; the martensitic transformation temperatures of various Fe- and U-based alloys and the metastable phase transformation diagrams of steels 20Kh13 and 30KhGSA cooled from various temperatures are plotted. The joint effect of Mo, Nb, and Zr on the martensitic transformation temperature is examined. The findings bear out the conclusion about the athermal dependence of the martensitic transformation temperature on the cooling rate of steel and the stabilizing effect of the cooling rate on austenite. Figures 2; references 11.

Investigation of Surface Layer's Chemical Composition and Diffusion Processes in Cu-Ni-Au System

937D0106E Moscow *METALLY in Russian No 1*, Jan-Feb 93 pp 141-145

[Article by S.I. Sidorenko, T.V. Litvinova, S.M. Voloshko, I.M. Klimachev, Kiev; UDC 669.3'24'21:532.72]

[Abstract] Extensive use of multilayer Cu-Ni-Au systems as microstrip lines and other elements in microelectronics and the negative impact of interdiffusion in such structures on their service life, reliability, and performance, as well as the lack of data on the diffusion processes in ternary systems prompted an examination of the diffusion processes in the multilayer Cu₁-Cu₂-Ni-Au composition on a polycr substrate (where the subscripts denote electrodeposited and vacuum-deposited layers). To this end, a stepped multilayer structure each of whose layers is accessible to analysis is investigated. The surface condition and effect of ionic bombardment on the system composition and structure are studied with the help of electron Auger spectroscopy. The behavior of the C, Cl, O, and Cu peak intensity in Auger spectra plotted on the electro- and vacuum-deposited Cu, Ni, and Au layers as a function of the ionic etching duration is plotted, and the behavior of the element concentration on the surface layer in the initial state, after etching, as well as after annealing and during ionic etching is summarized. The study shows that at temperatures above 673K, copper diffuses intensively

through the Ni and Au layers while nickel diffuses at a slower rate; moreover, the Cu, Ni, and Au layers produced by electrodeposition are contaminated with impurities, mostly C, whose concentration drops by tenfold after 600 s of ionic treatment. It is recommended that in making microstrip structures with subsequent thermal compression welding, the temperature should not rise above 600K; operation of microelectronic devices with a Cr-Cu-Ni-Au structure is not recommended at elevated temperatures; thermal compression welding must be preceded by gold surface cleaning to remove organic and inorganic impurities. Figures 3; tables 3; references 13: 3 Russian, 10 Western.

Radiation-Induced Processes in Metallic Alloys' Subsurface Layers

937D0106F Moscow *METALLY in Russian No 1*, Jan-Feb 93 pp 150-161

[Article by G.G. Bondarenko, Moscow; UDC 669.018.7:616-001.2]

[Abstract] Radiation-induced processes in the subsurface layers of metal alloys are investigated and their effect on the performance of structures and devices is considered. Attention is focused on the outcome of the interaction of accelerated particles fluxes with the metals' subsurface layers, i.e., the physical phenomena that greatly affect the surface properties and resistance to external factors. Such radiation-induced defects as blistering, flaking, sublimation, segregation, and sputtering are examined in detail. The kinetic sublimation curves of various types of steel and Al-Li alloys in a vacuum under irradiation, the temperature dependence of the lithium concentration in Li-Al alloys, the component distribution profiles in various alloys, and the dependence of the He-Ne mixture pressure in a test ampoule on the sputtering duration under irradiation are plotted. The findings are used for selecting materials for various devices operating under irradiation, e.g., reactor cores and pressure vessels. It is noted that although radiation-induced phenomena are regarded as undesirable, since actual alloys are developed for a specific range of properties determined by the chemical and phase composition that may change under irradiation, in some cases such phenomena may be used to improve the material's properties. Figures 12; references 24: 17 Russian, 7 Western.

New Compounds With YbMo₂Al₄ and Th₂Zn₁₇ Structure

937D0106G Moscow *METALLY in Russian No 1*, Jan-Feb 93 pp 210-212

[Article by B.M. Stelmakhovich, Yu.B. Kuzma, L.G. Akselrud, Lvov; UDC 669.018.3.715+546.736]

[Abstract] The new compounds were discovered in the neighborhood of Yb₁₅Cu₇₃Al₁₂ and Yb₁₁Cu₃₂Al₃₇ compositions while studying the phase equilibria diagram of the Yb-Cu-Al system. Their crystal structure is

examined. To this end, samples are fused from initial components with a varying degree of purity in an electric arc furnace in a purified Ar atmosphere on a water-cooled copper bottom. Diffusion annealing is conducted in evacuated quartz ampoules filled with Ar at 870K for at least 800 h. A phase analysis is carried out using Debye patterns, the Bragg angles and reflection intensity are determined by the diffraction patterns of powder in a DRON-3M diffractometer in CuK radiation using step-by-step intensity recording.

An X-ray pattern indication reveals that the new compound probably has a body centered tetragonal lattice. The atomic spacing and coordination numbers of atoms are summarized. The findings show that the $\text{YbCu}_{5.12}\text{Al}_{0.88}$ compound structure is similar to that of YbMo_2Al_4 and that the new lanthanide-based compound $\text{Ln}_2\text{Cu}_{10}\text{Al}_7$ where Ln = Tm, Yb, or Lu has a $\text{Th}_2\text{Zn}_{17}$ -type rhombohedral structure. In both compounds, the smaller atom has an icosahedral coordination. Tables 3; references 5: 4 Russian, 1 Western.

Electrochemical Synthesis of Tungsten and Molybdenum Borides in a Disperse State

937D0103A Kiev POROSHKOVAYA

METALLURGIYA in Russian No 1, Jan 93

(manuscript received 8 Oct 91) pp 8-11

[Article by Kh.B. Kushkhov, V.V. Malyshev, A.A. Tishchenko, and V.I. Shapoval, General and Inorganic Chemistry Institute, Ukraine Academy of Sciences, Kiev; UDC 541.135.3]

[Abstract] A study examined the electrochemical synthesis of tungsten and molybdenum borides from the melted mixture $\text{NaCl-Na}_3\text{AlF}_6\text{-Na}_2\text{Mo}_4(\text{MO}_3)\text{-B}_2\text{O}_3$ (where $\text{M} = \text{Mo}$ or W). Depending on the composition of the individual melt and electrolysis parameters, both individual boride phases of refractory metals (the higher boride MB_4) and a mixture of phases (including the lower borides M_2B , MB , MB_2 , and M_2B_3) were isolated. The electrolysis products were identified by X-ray phase analysis on a DRON-2 diffractometer with CuK_α radiation and a vanadium filter. When graphite was used as the anode material and the voltage in the pool did not exceed 2.5 V, the cathode precipitate consisted mainly of metallic tungsten and molybdenum. A phase mix (M , M_2B , MB , MB_2 , and M_2B_3) resulted on the cathode at voltages of 2.5 to 3.5 V, whereas at voltages of 3.5-4.5 V the precipitate consisted primarily of the higher boride MB_4 . Overall, the process of electrochemical synthesis of tungsten and molybdenum borides was determined by the following interconnected parameters: composition of the electrolyte bath, voltage in the bath, and electrolysis temperature and duration. The optimum melt composition was (mass percent) NaCl , 39.25-44.4; Na_3AlF_6 , 39.25-44.4; $\text{Na}_2\text{Mo}_4(\text{MO}_3)$, 1.0-1.5; and B_2O_3 , 10-20. A voltage of 3.5-4.5 V, process temperature of 900-950°C, and process duration of 45-60 minutes were found to be optimum. The yield of single-phase MoB_4 and WB_4 amounted to 0.2-0.3 and 0.3-0.45 g/A-h, and the final MoB_4 and WB_4 disperse powders had a specific surface of 5-15 m^2/g . Figure 1, table 1; references 7: 5 Russian, 2 Western.

Calculating Compaction Kinetics of Powder Amorphous Metal Materials in the Process of Hot Isostatic Compaction

937D0103B POROSHKOVAYA METALLURGIYA

in Russian No 1, Jan 93 (manuscript received

22 Aug 91) pp 12-16

[Article by V.A. Pozdnyakov and V.Ye. Vaganov, Central Scientific Research Institute of Ferrous Metallurgy, Moscow; UDC 621.762.4:539.213]

[Abstract] The kinetics of the compaction of powder amorphous metal materials under an applied pressure P in the temperature interval $T_p < T < T_k$ (where T_k represents crystallization temperature) were calculated, and a diagram of the process of hot isostatic pressing with the coordinates relative density-temperature-pressure was constructed. An 18-equation model was

developed on the basis of published data, and the compaction process was tentatively divided into two stages. The powder was assumed to consist of spherical particles of the same size that compacted in the initial stage. This was a result of the area S of near-contact necks between the material particles and their growing number as the particle radius increased and compacted in the second stage as a result of the spherical pores healing. The dependence of the deformation rate on stress was found to assume the form of a hyperbolic line. The model presented makes it possible to calculate diagrams of the mechanisms and kinetics of hot compaction of amorphous metal materials once the temperature dependences of viscosity, yield point, and incubation period of the onset of the crystallization of specific alloys have been calculated. The resultant calculations will in turn make it possible to predict optimal regimens for producing blocks of amorphous materials. Figures 2; references 14: 5 Russian, 9 Western.

The Structure and Properties of Iron-Based Alloys Sintered by the Method of Electrocontact Heating

937D0103C Kiev POROSHKOVAYA

METALLURGIYA in Russian No 1, Jan 93

(manuscript received 5 Nov 91) pp 33-40

[Article by L.O. Andrushchik, E. Dudrova, S.P. Oshkaderov, and M. Kabatova, Metal Physics Institute, Ukraine Academy of Sciences, Kiev, and Experimental Metallurgy Institute, Slovak Academy of Sciences, Koshitse, Czech and Slovak Federated Republic; UDC 621.762:539.214]

[Abstract] A study examined the structure, porosity characteristics, and mechanical properties of iron-based alloys sintered by high-speed electrocontact heating. The properties of the study alloys were then compared with those of their counterparts sintered by the classic furnace method. Alloys with two different compositions were studied. The first group contained the following (percent): C, 0.08; S, 0.011; Cr, 0.05; Mn, 0.29; Mo, 0.53; Ni, 1.92; and O_2 , 0.18. The second group of alloys contained the following (percent): C, 0.11; S, 0.028; Cr, 0.32; Mn, 0.52; Mo, 0.30; Ni, 0.25; and O_2 , 0.23. Graphite was added to each of the powdered mixtures and were compacted in air at pressures of 400, 600, and 800 MPa. The precompact study specimens were then sintered in a specially created experimental unit in a medium of extremely dry hydrogen by passing them directly through an electric current as described in another publication. Samples of the same two materials were also sintered by the classic method in a semi-industrial furnace in a regimen including heating at a rate of 16 K/min to a sintering temperature of 1,473 K for 50 min, holding at that temperature for 30 min, and cooling to room temperature for 80 min at a rate of 15 K/min. The specimens sintered by the electrocontact method were heated at a rate of 1,200 K/min and cooled at a rate of 250 K/min. The electrocontact sintering was performed at 1,373 K, 1,473 K, and

1,573 K with holding periods of 1, 5, 15, and 30 min. The classic furnace sintering was performed at the same temperatures with holding periods of 30 min. The structure and properties of the materials produced by the two sintering techniques were studied by hydrostatic weighing, metallographic microscopy, and scanning electron microscopy. High-speed electrocontact heating resulted in significant process activation that in turn resulted in significant time savings compared with classic furnace-based sintering. High-speed electrocontact sintering resulted in alloys with increased density, decreased porosity, and better pore structure. Metallographic and fractographic studies established the occurrence of local temperature increases at the interparticle contacts that resulted in the formation of a liquid phase at the said sites. The formation of larger compounds resulted that were both structurally and geometrically more perfect. The liquid metal enveloped the pores' surfaces, made them smooth, filled in their irregularities, and closed their channels. As a result, the pores became smaller and assumed a spherical shape. Consequently, the electrocontact-sintered specimens had better mechanical properties than did their furnace-sintered counterparts. Figures 3, tables 4; references 11: 9 Russian, 2 Western.

Magnesium-Phosphate Self-Hardening Sands

937D0024A Moscow LITEYNOYE PROIZVODSTVO
in Russian No 6, Jun 92 pp 10-11

[Article by S. I. Rivkin and Ye. N. Yurginson, Izhora Plant Production Association, and L. G. Sudakas and L. I. Turkina, State Scientific Research and Planning Institute of the Cement Industry; UDC 621.742.48]

[Abstract] The experience with use of magnesium-phosphate self-hardening foundry sands for large and medium-size steel castings at the Izhora Plant Production Association is described. Cores are made of silica and zircon-based magnesium-phosphate sands weighing from 4 kg and 4 tons, with a total annual production of 3,000 tons in the association's foundry. Magnesium-phosphate sands can be combined with sands with water-glass and synthetic-resin binders for use as facing and filler sands. The magnesium-phosphate self-hardening sands contain three primary groups of substances: an active component (binder) consisting of a magnesium powder component and a phosphate liquid component; a filler (sand) that provides certain thermal, gas-dynamic and contact properties; and modifier additives that provide necessary hardening conditions. Thanks to high binding capacity of the magnesium-phosphate mixture, the total amount of magnesium-containing powder and liquid component is only 3-5%. The low content of the active component in these sands makes core knock-out easy to perform with conventional methods such as knock-out grids and by hand.

Quality of Sand from Tolmachevo Evaluated

937D0024B Moscow LITEYNOYE PROIZVODSTVO
in Russian No 6 Jun 92 pp 11-12

[Article by Yu. F. Borovskiy, I. V. Shergin, and Yu. N. Zinin, Northwest Correspondence Polytechnical Institute; UDC 621.742.85]

[Abstract] Sand from the Tolmachevo quarry was evaluated for its potential as a substitute for Lyubertsy sand, which is the core sand of choice at the "Zvezda" Plant in St. Petersburg for casting aluminum diesel blocks and manifold parts. The mineral content of the sands was determined by the x-ray diffraction method. Strength tests of cores made of the two different sands and using three different binders showed that Tolmachevo sand cannot qualify as a full-fledged substitute for Lyubertsy sand. Used core sand from Tolmachevo and a shop mixture of the two sands were reclaimed on a dry mechanical unit, and the reclaimed products were also treated in a "pseudo-fluidized bed" unit. Tests of the reclaimed products showed that they can be used as a partial substitute for Lyubertsy sand.

Making Casting Molds Using Vibration Methods

937D0024C Moscow LITEYNOYE PROIZVODSTVO
in Russian No 6, Jun 92 pp 12-14

[Article by A. A. Brechko and A. V. Sokolov, Foundry Machinery Institute; UDC 621.742.4]

[Abstract] A promising way of improving the process of making large molds and cores of sodium silicate and resin sands is to reduce the surface energy and viscosity of the binder with the aim of efficiently distributing filler among the grains and to reduce internal stresses in the binder. Molding sands with a minimum binder content are characterized by high mobility, which allows vibration methods of compaction to be used for making molds and cores with low energy costs. Sodium silicate sands with a plasticizing additive were tested for three conventional hardening methods: the CO₂ process, fast drying with heat, and cold hardening with solid and liquid hardeners. In all three methods the use of a plasticizer was effective in allowing less binder to be used while maintaining desirable strength and friability properties. In sands with furan resins, binder content was reduced by lowering the binder's viscosity and surface energy. The best result was achieved by using a monomer plasticized with a polymer as the base.

Molds made of the sands with reduced binder content were compacted by vibration in the vertical and horizontal directions on test benches to study the effect of vibration on disperse systems (quartz sand + binder). It was found that a mold structure obtained by horizontal vibration compaction is the most efficient, providing maximum structural strength. This method allows for minimum energy expenditure for compaction per unit weight of sand, and allows molds to be made in a wide range of weights.

Casting of Aluminum-Based Composites With Crystallization Under Pressure

937D0024D Moscow LITEYNOYE PROIZVODSTVO
in Russian No 6, Jun 92 pp 14-16

[Article by N. N. Belousov, Institute of Mechanics; UDC 621.74.043.2:669.715]

[Abstract] In conventional gravity casting of composite material parts, there can occur sedimentation of hardeners, which leads to local coarsening and the development of liquation processes. One way of preventing this is the method of casting with crystallization under pressure (forging of molten metal), which was developed in St. Petersburg under the direction of V. M. Plyatskoy. Aluminum alloy-based composites made by one of two established methods (vortex process, in which powders or fibers of refractory metals, carbides, nitrides, etc. are mixed intensively in the molten metal; or plasma injection, in which the hardeners are introduced with a plasma jet of an inert gas) are cast into steel molds mounted on hydraulic presses.

This process was used to produce test lots of internal-combustion engine pistons made from the composite "Altik". Metallographic studies of the pistons showed a high density and fine-grain structure of the composite, with hardeners distributed uniformly. Study of mechanical properties showed decreased ductility as the content of titanium or intermetallic compounds increased, as well as increased strength at temperatures up to 300-350°C. The process was also used to make mold inserts for injection-molding machines. Studies showed that the wear resistance of inserts made of composites is much higher than that of inserts made of steel when used in injection molding of glass-fiber-reinforced plastics.

Making Castings of Metal-Base Composites

937D0024E Moscow LITEYNOYE PROIZVODSTVO
in Russian No 6, Jun 92 pp 16-17

[Article by V. G. Borisov, Scientific and Production Association "All-Union Institute of Aluminum and Magnesium"; UDC 621.74.011:669.715]

[Abstract] A method of making cast aluminum-base composites is described in which structure formation is controlled by adding particles of an intermetallic compound to the molten base metal when its temperature is in the range between the liquidus and solidus curves. For example, if iron is added to molten aluminum in the form of particles of the intermetallic Al_3Fe , within the liquidus-solidus range the degree to which the particles dissolve will be determined by the temperature of the melt, the size of the particles, and the time that they are in the melt. Also, intermetallic compounds having a different stoichiometry (e.g., Al_3Fe_2) can affect the thermodynamics of the process because of their different properties. In the system Al-Ti, there are nine types of Al and Ti compounds with differing stoichiometry, crystal lattice types and parameters, and physicochemical properties. Use of these compounds

makes it possible to obtain alloys of the same general chemical composition but with widely varying structures and mechanical properties.

To implement the method, the intermetallic compound is added in the form of a powder to the melt in a reactor equipped with a device for batching, heating and ionic pickling of the surface of added particles, and a crucible with a device for mixing the melt as the compound is added. This equipment and technology for forming the produced composites were developed at the Scientific and Production Association "All-Union Institute of Aluminum and Magnesium". Materials have been produced that are tens of times more wear-resistant than known alloys and possess a higher modulus of elasticity, strength and other properties. Composites based on Al-Si alloy have been produced with a SiC content of up to 20%. In them, strength and ductility properties are retained while increasing the modulus of elasticity (to 85 MPa), with wear resistance increased by dozens of times.

Ceramic Molds for Relief Surface Castings

937D0024F Moscow LITEYNOYE PROIZVODSTVO
in Russian No 6, Jun 92 pp 18-20

[Article by F. D. Obolentsev, Yu. A. Kaplunovskiy, and L. M. Mirson, All-Union Planning and Technological Institute of Casting Machinery Manufacture; UDC 621.74.045]

[Abstract] Processes for making ceramic molds for castings with relief surfaces are described. Molds made by these processes include cores made of a sand and sodium silicate mixture which are ceramic-coated using a gelled suspension poured around the cores inside engraved plaster boxes; shells made of a quartz-water slip poured around a plaster core inside an engraved plaster box; and shells made of hot suspensions such as molten quartz which are pressed into plaster boxes, and after setting the shells are removed and sprinkled with aluminum oxide and fired up to 1000°C for solid-phase sintering of the refractory material. Also described is a process for making molds with coordinated engraving on a core.

Combined Method of Manufacturing Gas Turbine Rings

937D0024G Moscow LITEYNOYE PROIZVODSTVO
in Russian No 6, Jun 92 pp 20-21

[Article by A. G. Kovalev, A. N. Lemesko, and N. V. Levnikov, "Neva Plant" Production Association; UDC 621.74.002.6:669.14]

[Abstract] Results of casting gas turbine rings by two different methods are reported. One method involves investment casting of separate sections of a ring in ceramic molds heated to 900°C, and the other involves casting of the whole ring in a metal mold. The weight of each cast ring section was 60 kg, and the weight of the wholly cast ring was 1500 kg with a wall thickness of 82-108 mm. Heat treatment of the castings consisted of

cooling from 1200°C for 3 hours, quenching in water, followed by ageing at 800°C for 10 hours.

Tests of mechanical properties of the castings showed that the metal cast in ceramic molds had lower ductility and impact strength, whereas the metal cast in a metal mold had mechanical properties on a par with those of gas turbine rings manufactured by the traditional forging method. Tests of the castings for long-term strength showed that the long-term ductility of the metal cast in a metal mold was twice that of the metal cast in ceramic molds. As a result, a process has been developed and introduced for manufacturing castings for gas turbine rings from TsZh-13L steel to replace forgings, which increases the yield of fit metal by 30% and saves labor costs.

Doping $\text{Bi}_2\text{Te}_{2.85}\text{Se}_{0.15}$ Solid Solution with Tellurides of Yttrium (Y_2Te_3) and Gadolinium (Gd_2Te_3)

937D0095C Moscow NEORGANICHESKIYE MATERIALY in Russian Vol 29 No 2, Feb 93 pp 190-192

[Article by T. Ye. Svechnikova, S. N. Chizhevskaya, N. M. Maksimova, P. P. Konstantinov, G. T. Alekseyeva, and O. D. Chistyakov, A. Baykov Institute of Metallurgy, Russian Academy of Sciences; UDC 546.87'24'23:66.046.516]

[Abstract] The effect of doping of $\text{Bi}_2\text{Te}_{2.85}\text{Se}_{0.15}$ solid solution with tellurides of yttrium (Y_2Te_3) and gadolinium (Gd_2Te_3) on thermoelectric and mechanical properties was investigated. Doped crystals were obtained by the Czochralski and Bridgman processes. The effective coefficient of distribution of yttrium in this solid solution was calculated to be 0.15.

It was demonstrated that doping results in lower electrical conductivity and thermoelectric efficiency of the material. It was determined that the dependence of the material's bending strength on concentration of the doping agent has a monotone character, which is associated with a change in the mechanism of dissolving of Y_2Te_3 .

Production and Properties of $\text{Ag}_{0.12}\text{Ga}_{0.12}\text{Ge}_{0.88}\text{Se}_2$ Single Crystal

937D0109A NEORGANICHESKIYE MATERIALY in Russian Vol 29 No 5, May 93 (manuscript received 26 Jun 92) pp 617-619]

[Article by I.D. Olekseyuk, G.Ye. Davidyuk, N.S. Bogdanyuk, A.P. Shavarova, V.V. Bozhko, G.P. Gorgut, and A.F. Lomzin, Luts'k State Pedagogical Institute imeni L. Ukrainka; UDC 541.123.2]

[Abstract] Large single crystals of birefringent $\text{Ag}_{0.1}\text{Ga}_{0.1}\text{Ge}_{0.9}\text{Se}_2$ solid solution were experimentally produced under controlled conditions from a mixture of 999.9% pure silver, 99.997% pure gallium, 40/3.0 germanium single crystals, and extra-pure 22-4 selenium. Synthesis of these ingredients took place in quartz containers at one temperature not higher than 1250 K under a vacuum of 0.01 Pa, with mixing by the vibratory method, and was followed by isothermal annealing at 870 K for 240 h. The product of this treatment was a dark-red compact with a range of optical transparency much wider than those of its ingredients. The conditions for growing single crystals were selected on the basis of the constitution diagram obtained by differential thermal analysis and tensiometry. Melting of the $\text{Ag}_{0.1}\text{Ga}_{0.1}\text{Ge}_{0.9}\text{Se}_2$ phase was found to begin at 978 K and end at 998 K, with a slight 5-10 K supercooling during crystallization and its dissociation taking place at temperatures above 700 K, as indicated by formation of a permanent film of dissociation products on the manometer surface. Single crystals were grown by the Czochralski-Bridgman method in specially designed containers: temperature in the melting zone 990-1200 K and in the annealing zone 750 K, temperature gradient in the crystallization zone 3-5 K/mm, growth rate 0.2-0.6 mm/h, annealing time 150 h, cooling rate 5 K/h. Eutectic crystallization was found to take place during the final stage of the process, this part of the crystal occupying 20-30% of the total volume and the remainder being a dark-red $\text{Ag}_{0.12}\text{Ga}_{0.12}\text{Ge}_{0.88}\text{Se}_2$ single crystal. Optical and electrical properties of these single crystals were determined on 0.05-5 mm thick ones. Their absorption spectra were measured with an alternating signal first passed through a narrow-band amplifier and afterwards picked up by a synchronous detector. They were found to be transparent, with a transmission coefficient $T = 1.0$, for all radiation on the longer-wave side of temperature-dependent steep edge (0.56 μm at 291 K) and to absorb all radiation on the shorter-wave side of this edge. Their absorption coefficient k was measured at temperatures $T = 77-480$ K and found to depend on the temperature as well as on the quantum energy of incident radiation, with $k_{\text{max}} = 900-1000 \text{ cm}^{-1}$ at the edge of the fundamental absorption band at all temperatures. The electrical properties of these single crystals was measured at temperatures $T = 200-400$ K. They were found to have a very high electrical resistance (1000 $\text{M}\Omega\cdot\text{cm}$ at 291 K), an exponentially temperature-dependent electrical conductivity $\sigma = 5e^{-E/2kT} \text{ kS/cm}$ (thermal energy of conductivity activation $E = 1.38-1.42 \text{ eV}$), and a linearly temperature-dependent width of the energy gap $E_g = E_{g,77\text{K}} - \alpha T$ ($\alpha = 0.0013 \text{ eV/K}$, $E_{g,77\text{K}} = 2.47-2.51 \text{ eV}$ at 77 K and 2.24-2.28 eV at 291 K). Scattering of incident 0.63 μm light by these single crystals revealed their imperfection, the intensity distribution pattern of the scattered light indicating the presence of inhomogeneities larger than that wavelength. Figures 7; references 8.

Electronic Structure and Optical Properties of ZrO_2 stabilized with Yttrium

937D0109B Moscow NEORGANICHESKIYE MATERIALY in Russian Vol 29 No 5, May 93 (manuscript received 12 Feb 92) pp 636-640

[Article by G.A. Olkhovik, I.I. Naumov, O.I. Velikokhatnyy, and N.N. Aparov, Institute of Strength Physics and Materials Science in Siberian Department, Russian Academy of Sciences; UDC 538.915:539.2: 546.514.9]

[Abstract] A comprehensive study of the $(\text{ZrO}_2)_6 \cdot \text{Y}_2\text{O}_3$ complex, cubic zirconia stabilized by yttrium ions, containing 24 atoms and one oxygen vacancy of ZrO_2 was made concerning its electronic structure, its optical properties, and the stabilization mechanism. The density of electronic states and the electron energy spectrum were measured covering the 10-30 eV range. Analysis of the data and theoretical calculations indicate that the complex is a dielectric material which, owing to formation of an 1s-vacancy band in it, has an energy gap much narrower than that of pure zirconia. The possibility of electronic transitions into the 1s-vacancy band is evidently responsible for making the optical properties of the complex appreciably different than those of pure zirconia. This is revealed by the frequency (energy quantum) spectrum of the electric susceptibility (imaginary part of dielectric permittivity ϵ_2), the reflection coefficient R for normally incident electromagnetic waves, and of factor L representing the characteristic energy loss by fast electrons. Stabilization has shifted the edge of optical absorption to a lower frequency while anomalously boosting those other three optical properties at frequencies somewhat above that edge. The results of this study confirm the hypothesis that stabilization of cubic zirconia by yttrium ions is due principally to weakening of the Coulomb attraction between the oxygen ions. Figures 6; tables 1; references 8.

Determining Possibility of Superconductivity in $\text{La}_{2-x}(\text{M}^{2+} = \text{Ca}, \text{Sr}, \text{Ba})_x\text{Cu}_2\text{O}_6$ on Basis of Their Electronic Structure

937D0109C Moscow NEORGANICHESKIYE MATERIALY in Russian Vol 29 No 5, May 93 (manuscript received 5 Jun 92) pp 648-651

[Article by V.P. Zhukov, Institute of Solid-State Chemistry in Urals Department, Russian Academy of Sciences; UDC 546.261]

[Abstract] The possibility of superconductivity in high- T_c $\text{La}_{2-x}(\text{M}^{2+} = \text{Ca}, \text{Sr}, \text{Ba})_x\text{Cu}_2\text{O}_6$ with $x > 0.14$ is considered, at least those with $x < 0.14$ having been found to be metal-like but not superconducting. On the premise that this possibility is determined by the electronic structure, pertinent calculations have been made for a simple tetragonal crystal by the semiempirical strong-link method in the basis of atomic Slater

orbitals (4sCu, 4pCu, 3dCu, 2sO, 2pO, 6sLa, 6pLa, 5dLa). The orbital parameters, the atomic populations, and the Fermi level were averaged over 40 k-vectors uniformly distributed over the irreducible part of the Brillouin zone. The effect of substituting bivalent Ca, Sr, Ba atoms for trivalent La atoms was, in accordance with the "rigid bands" model, evaluated by first appropriately changing the total number of electrons in the unit cell. The results indicate that the La-Ca-Cu-O, La-Sr-Cu-O, La-Ba-Cu-O compounds with $x = 0.5$ will probably be high-temperature superconductors. Figures 3; tables 2; references 12.

Possibility of Cold Nuclear Fusion at Temperature of Ferroelectric Phase Transition in KD_2PO_4

937D0109D Moscow NEORGANICHESKIYE MATERIALY in Russian Vol 29 No 5, May 93 (manuscript received 10 Dec 92) pp 656-658

[Article by V.B. Kalinin, Institute of Physical Chemistry at Russian Academy of Sciences; UDC 548.736.5]

[Abstract] As a compound suitable for "cold" nuclear fusion at the temperature of the target is being proposed the KD_2PO_4 potassium phosphate, which features split D-positions and a reversible transition of the first kind from its low-temperature, low-density ferroelectric phase to its high-temperature, high-density paraelectric phase at about 221 K. This transition is attributed to fusion of two D-positions into one. It can take place not only during heating-cooling cycles, but also under rising pressure. In an experiment with this compound, whose Curie phase transition temperature lies within the 219-223 K range, most neutrons were recorded at 221 ± 0.3 K and 222 ± 0.3 K. According to available data, the mechanism of cold nuclear fusion is evidently the interaction of two deuterons with lattice excitation initiated by that phase transition. This interaction produces a proton (p), tritium (T), and a virtual gamma quantum γ , which then yields $T + p$ and ${}^3\text{He} + n$. Three possible effects stimulating the population of neighboring positions at the phase transition temperature and consequently cold fusion of D nuclei are:

(1) The breakup of the KD_2PO_4 crystal into domains at that temperature with an attendant step increase of electric polarization and thus of the electric field intensity inside each domain up to 100 MV/cm necessary for accelerating the deuterons;

(2) The impediment of the relaxation of charge and field fluctuations which arise, below and above the Curie temperature, owing to the low mobility of domain walls (six orders of magnitude lower than the mobility of domain walls in KH_2PO_4);

(3) The "softening" of lattice vibrations near the Curie temperature. Figures 2; references 15.

Chemical Structure Specifics and Optical Properties of Sulfur-Enriched As-S-Ge Glasses

937D0109E Moscow NEORGANICHESKIYE MATERIALY in Russian Vol 29 No 5, May 93
(manuscript received 28 May 92) pp 689-691

[Article by D.I. Tsiulyanu, Kishinev Polytechnic Institute imeni S. Laso, and N.A. Gumenyuk, Institute of Applied Physics at Moldovan Academy of Sciences; UDC 539.21.213]

[Abstract] An experimental study was conducted on the interrelation between the chemical structure of AsS_3 - GeS_4 glasses with a catenolaminate ($r\text{-dash} \leq 2.67$) structure and on their optical properties at the edge of the fundamental band. Such glasses were produced by the synthesis of AsS_3 ($r\text{-dash} = 2.4$ and GeS_2 ($r\text{-dash} = 2.666$), the average number of covalent bonds per atom in these compounds having been increased by increasing the concentration of either As or Ge. Thin layers of these glasses were grown by discrete thermal deposition on optical glass or quartz substrates under a vacuum of 1 mPa. The density of the materials was measured by weighing in toluene. The vibrational light transmission spectra of specimens molded into polyethylene were measured with an FIS-3 two-beam spectrometer over the 400-33 cm^{-1} range. The results of transmission and reflection measurements made for layers of various thicknesses were used for calculating the absorption coefficient α at the edge of the fundamental band. The optical width of the energy gap was calculated by extrapolation of $(\alpha \text{ hv})^{1/2} = f(\text{hv})$ curve to the magnitude of photon energy hv , which corresponded to $(\alpha \text{ hv})^{1/2} \rightarrow 0$. Increasing $r\text{-dash}$ was found to either appreciably narrow or widen the energy gap, depending on whether $r\text{-dash}$ was being increased by increasing the concentration of Ge atoms with the coordination number 4 in the AsS_3 - GeS_4 mixture and further to pure GeSe_2 or by increasing the concentration of As atoms with coordination number 3 respectively. The elastic constants of these glasses are already known to be very small and almost independent of the average number of covalent bonds per atom. As the GeS_4 concentration is increased, evidently Ge atoms replace As atoms, and the average number of covalent bonds per atom thus increases while the laminate intermediate-order topological structure is retained. The attendant change of the molar volume is essentially due to changing interaction of unshared electron pairs, interaction on which the width of the optical gap depends, and consequently also changing intermolecular or interlaminar distance. Figures 3; references 5.

Mechanism of $\text{YBa}_2\text{Cu}_3\text{O}_{7-x}$ and $\text{Ca}_2\text{Sr}_2\text{Bi}_2\text{Cu}_3\text{O}_{10-x}$ by Nitrogen Oxides according to Electron-Paramagnetic Resonance Data

937D0109F Moscow NEORGANICHESKIYE MATERIALY in Russian Vol 29 No 5, May 93
(manuscript received 26 Mar 92) pp 700-703

[Article by E.F. Saakyan, A.A. Muradyan, and T.A. Garibyan, Institute of Chemical Physics at Armenian Academy of Sciences; UDC 538.945:546.17]

[Abstract] An experimental study of ceramic high-temperature $\text{YBa}_2\text{Cu}_3\text{O}_{7-x}$ and $\text{Ca}_2\text{Ba}_2\text{Bi}_2\text{Cu}_3\text{O}_{10-x}$ was made by the EPR (electron-paramagnetic resonance) method concerning their interaction with nitrogen oxides NO and $\text{NO}_x = \text{NO} + (\text{NO}_2 \text{ in air})$. Two specimens (I,II) of Y-Ba-Cu-O ceramic and one specimen (III) of Ca-Sr-Bi-Cu-O ceramic had been obtained for this experiment: specimen I (specific surface 0.1 m^2/g and critical temperature 91 K) by self-propagating synthesis, specimen II (specific surface 0.1 m^2/g and critical temperature 89 K) by conventional technology, and specimen III (critical temperature 98 K) also by conventional technology. Their degradation was monitored on the basis of EPR A-,C-,D-signals transmitted by paramagnetic Cu^{++} ions and Cu^+ ions, also on the basis x-ray phase analysis. The pressure on all specimens, initially under a vacuum of about 1.3 Pa, was raised by injection of NO alone (27 kPa) or of NO (27 kPa) + air (62.5 kPa). All specimens were tested at 298 K room temperature for 24 h and then at higher temperatures for 2-3 h. At room temperature both Y-Ba-Cu-O specimens retained their superconductivity almost totally in an NO atmosphere, but in an $\text{NO} + \text{air}$ atmosphere, the formation of $[\text{Cu}^{++}\text{NO}_2^-]$ complexes indicated the presence of Cu^+ ions in them. Degradation of this ceramic in an NO, NO_2 atmosphere began at 473 K and continued at temperatures up to 673 K (specimen I) or up to 773 K (specimen II) without formation of the intermediate phases BaCuO_2 and Y_2BaCuO_5 , the latter phase being formed only as a result of mechanical crushing. The specimen of Ca-Sr-Bi-Cu-O ceramics retained its superconductivity in an NO, NO_2 at temperatures up to 823 K, at which its degradation began. Figures 4; references 12.

Solid Solution $\text{Y}_{1-x}\text{Ln}_x\text{Ba}_2\text{Cu}_3\text{O}_{7-y}$ ($\text{Ln} = \text{Ce}, \text{Pr}, \text{Tb}$)

937D0109G Moscow NEORGANICHESKIYE MATERIALY in Russian Vol 29 No 5, May 93
(manuscript received 20 Feb 92) pp 735-736

[Article by V.V. Zelentsov, T.N. Fesenko, M.B. Varfolomeyev, and V.Yu. Stozhkov, Moscow Institute of Engineering Physics; UDC 533.312.62]

[Abstract] An experimental study on the superconductivity of $\text{Y}_{1-x}\text{Ln}_x\text{Ba}_2\text{Cu}_3\text{O}_{7-y}$ ($\text{Ln} = \text{Ce}, \text{Pr}, \text{Tb}$) ceramics was conducted. Although these ceramics with yttrium are known to be high-temperature superconductors when they are partly replaced by any of the three lanthanide elements Ce, Pr, Tb, those completely replaced by any of them are not. Pure 1-2-3-phase ceramics with $x = 0.1-0.3$ (Ce, Pr) and with $x = 0.1-0.15$ (Tb) were produced by a solid-phase reaction of the $\text{Y}_2\text{O}_3 + \text{BaO} + \text{CuO}$ mixture with BaLnO_3 ($\text{Ln} = \text{Ce}, \text{Pr}, \text{Tb}$) oxidizer at 820°C (Ce), 920°C (Pr), 940°C (Tb) for 3-5 h. Each of the three oxidizers was produced by thermal decomposition of the stoichiometric mixture of Ba and Ln nitrates at 1000-1100°C within 3 h. The mixture of Ba and Ce nitrates had been obtained by dissolution of both BaO and CeO_2 oxides in HNO_3 , with H_2O_2 also present so that the reaction $2\text{CeO}_2 + 6\text{HNO}_3 + \text{H}_2\text{O}_2 \rightarrow 2\text{Ce}(\text{NO}_3)_3 + 4\text{H}_2\text{O} + \text{O}_2$ could take place. The mixtures of Ba and

either Pr or Tb nitrates were produced by dissolution of their oxides in HNO_3 concentrate, followed by evaporation and drying. The three BaLnO_3 oxidizers were identified on the basis of x-ray phase analysis. The state of Pr^{++++} and Tb^{++++} ions was determined on the basis of their effective magnetic moment. X-ray diffraction analysis was performed in a deWolf camera (Enraph-Nonius, Holland) with a CuK_α -radiation source and a quartz monochromator, with 99.999% pure metallic Ge serving

as the internal standard. Magnetic susceptibility was measured by the Faraday method on an automated magnetic balance. The results indicate that, with $x(\text{Ce}, \text{Pr}) = 0.3$ and $x(\text{Tb}) = 0.15$, the solid-phase reaction with BaLnO_3 results in complete reduction of Ln ions to Ln^{+++} so that holes can form in the Cu-O planes. The superconducting phase thus forms when yttrium is replaced by $x = 0.1-0.3$ Ce and by $x = 0.1-0.17$ Pr or Tb. Tables 1; references 11.

Effect of Electrohydropulse Treatment (EGIO) on Metallic Melt Properties

937D0112B Moscow METALLY in Russian No 3,
May-Jun 93 pp 17-20

[Article by G.S. Yershov, V.I. Klichanovskiy, B.I. Butakov, G.V. Gavriluk, Kiev; UDC 669.046:621.746]

[Abstract] Extensive uses of melt treatment for improving the metal quality, e.g., electromagnetic and pulse stirring, pneumatic oscillation, ultrasonic treatment, and low-frequency vibration, prompted the development of a method of external dynamic treatment of the melt or solidifying ingot—the electrohydropulse treatment (EGIO)—employing the energy of electric discharge elastic vibration generators as the agent. The method developed at the Pulse Process and Technology Institute at the Ukrainian Academy of Sciences is characterized by a high instantaneous power (1-10 mW), a steep shock pulse leading edge, and a broad frequency spectrum. The effect of electrohydropulse treatment on the properties of metallic melts, e.g., such structure-sensitive characteristics as surface tension and viscosity, and the diffusion parameters of liquid steel, pig iron, and copper are investigated. To this end, steel and pig iron commercially smelted using electrohydropulse treatment and M0 copper with a total of 0.012% impurity content are examined. The chemical content of grey cast iron and steel 08GDNFL before and after electrohydropulse treatment is summarized; the effect of electrohydropulse treatment on the kinematic viscosity and surface tension (before and after) of steel 08GDNFL, grey cast iron, and copper M0 is plotted. The elements' diffusivity in liquid copper before and after electrohydropulse treatment is found experimentally. The findings demonstrate an increase in surface tension (4-5% for grey cast iron, 7% for steel, and 4-5% for copper) with a simultaneous decrease in kinematic viscosity (6-7% for steel, 9-10% for grey cast iron, and 15-16% for copper) as a result of electrohydropulse treatment and a considerable (by 1.2-2.5 times) acceleration of the elements' diffusion rate in copper. This is attributed to a decrease in the chemical microheterogeneity of the melts due to the breakup and shrinkage of clusters. Figures 2; tables 2; references 6.

Oxidized Metal and Alloy Behavior Characteristics Under Electron Bombardment Conditions

937D0112F Moscow METALLY in Russian No 3,
May-Jun 93 pp 101-105

[Article by G.G. Bondarenko, A.P. Korzhavyy, V.I. Kristya, A.M. Rozhkov, Moscow and Kaluga; UDC 621.9.048.7]

[Abstract] Expanding uses of sandwich structures formed by oxide films on the surface of metals and alloys, particularly Al, as electron sources in vacuum devices with a high secondary emission ratio (KVEE) within a broad bombarding electron energy range are discussed, and the nonuniform thickness of the 5-100

nm oxide film resulting in uneven surface charging is noted. To clarify the outlook for using oxidized metal and alloy samples as secondary emission cathodes (VEK) in electronic devices, the effect of the variable thickness oxide film on the electron movement near the bombarded surface is investigated theoretically. A vacuum diode formed by a secondary electron collector, a secondary electron cathode is considered, and the movement of electrons is described by a system of rate equations for the primary and secondary electron distribution functions and equations of electric field potentials. The findings confirm that the AD1 aluminum and Al-Cu-Mg alloys are a promising material for use in electronic devices if prior to oxidation, they are subjected to finishing rolling in "mirror" rolls to ensure their low roughness. References 7: 6 Russian, 1 Western.

Radiation Heat Treatment of Steel

937D0112G Moscow METALLY in Russian No 3,
May-Jun 93 pp 106-112

[Article by Yu.I. Gofman, Kharkov; UDC 621.9.048.7]

[Abstract] Radiation heat treatment (RTO)—a new waste-free and resource saving technology used in making metals and metal products with the help of a beam of relativistic electrons—is reviewed on the basis of numerous published sources. Radiation heat treatment is capable of penetrating the product up to 10 mm or more and heating the irradiated metal not from the surface, as in other heat treatment practices, but throughout the entire penetration depth. The relative capabilities of radiation heat treatment, electron beam treatment (ELO), and laser treatment (LO) are compared, and the dependence of the relative microhardness of steel 08Yu on the treatment temperature at a varying fluence and after model heat treatment and line diagrams (X-ray diffraction patterns) of transformer steel after radiation heat treatment and conventional heat treatment are plotted. The behavior of the mechanical and magnetic properties and microstructure under various types of heat treatment is discussed, and the conclusion is drawn that radiation heat treatment is promising for commercial use due to the availability of various electron accelerators. It is noted that radiation heat treatment is expedient in making thin rolled sheets and improving the operating properties of metallurgical equipment and cutting tools, as well as surface hardening. The author is grateful to I.I. Zalyubovskiy, I.V. Frantsenyuk, L.I. Frantsenyuk, I.V. Mizik, T.A. Kovalenko, T.F. Sukhov, and A.L. Samsonik for their help and support. Figures 3; tables 1; references 20.

Effect of Heat Treatment on Uniform Elongation of Medium Carbon Steel

927D0225A Moscow METALLOVEDENIYE I
TERMICHESKAYA OBRABOTKA METALLOV
in Russian No 7, Jul 92 pp 6-7

[Article by A. A. Azarkevich, A. A. Pashchenko, and T. A. Yevtukhova, Ukrainian Research Institute of Metallurgy; UDC 669.14.018.298.3:621.785.796]

[Abstract] The possibility of replacing 35KhGSA medium carbon steel with 35GSR steel for making connectors for attaching the paddles to chains in flight conveyors was investigated. Connectors made of 35KhGSA steel do not meet industry standards for breaking load and elongation. To determine whether 35GSR steel is a suitable replacement, it was of interest to investigate how uniform elongation of the steel depends on its heat treatment conditions and strength properties.

Cylindrical specimens were made out of heat-treated billets of 35GSR steel with different carbon contents, and they were tested on a tension machine. Together with relative elongation and reduction in area, uniform elongation was determined according to tension plots and, for comparison, according to the diameter of specimens after breaking. The character of the dependence of strength and plastic properties on the tempering temperature for specimens with different carbon contents was found to be identical. When tempering temperature is increased from 300 to 550 degrees C, strength characteristics decrease monotonically.

Analysis of the effect of heat treatment conditions on uniform elongation of 35GSR steel showed that the tempering temperature of connectors can be decreased to 300-350 degrees C, with an increase in their strength properties at values of uniform elongation which meet industry standards for residual deformation.

Oxidation of Pipe During Combined Furnace and Induction Heating

927D0225B Moscow METALLOVEDENIYE 1
TERMICHESKAYA OBRABOTKA METALLOV
in Russian No 7, Jul 92 pp 8-9

[Article by A. A. Zgura, O. T. Nikolskaya, T. V. Ivanova, and I. S. Stefanskiy, All-Union Research Institute of Pipes, Dnepropetrovsk; UDC 621.774:621.78.012]

[Abstract] The degree of oxidation of carbon steel pipe in the combined furnace and induction heating method was investigated with furnace heating first followed by induction heating, and vice versa. The degree of oxidation was also determined for both furnace and induction heating separately.

It was found that in the combined method with furnace heating first followed by induction heating, with the pipe heated to 400-600 degrees C in the furnace, the degree of oxidation of the metal is minimal (0.5-0.55% of the weight of the pipe). Furnace heating above 600 degrees followed by induction heating increases oxidation of the metal to 0.9%. With induction heating alone, oxidation of the metal is practically identical to oxidation in combined heating with the furnace first followed by induction heating, which demonstrates the advantage of the combined method (less electricity consumed than in straight induction heating). Combined heating with induction first followed by furnace heating has the

highest degree of oxidation, and this method is recommended only for installations that have a shielding gas atmosphere.

Electron Beam Treatment of Bearing Steels

927D0225C Moscow METALLOVEDENIYE 1
TERMICHESKAYA OBRABOTKA METALLOV
in Russian No 7, Jul 92 pp 13-17

[Article by A. A. Shulga, Taganrog Radiotechnical Institute; UDC 621.9.048.7:669.018.24]

[Abstract] The effect of the initial state of the metal and of electron beam treatment parameters on formation of a hardened layer in the bearing steels ShKh15 and ShKh15SG and the carburized steel 15G1 was investigated. Specimens of these steels underwent different heat treatments prior to electron beam treatment. The initial structure of pre-annealed steels ShKh15 and ShKh15SG was granular pearlite, and after undergoing oil hardening from 840 degrees C and tempering at 150 degrees C for two hours, the structure was fine-crystalline martensite, retained austenite (up to 5%), and finely dispersed carbides. Specimens of 15G1 underwent gas carburizing, oil hardening and tempering at 160 degrees C for two hours. The thickness of the carburized layer was about 1.5 mm. Electron beam treatment was done with a ribbon beam 0.5-2.0 mm thick and 40 mm wide and having a power of 1,000-50,000 W per square centimeter. The beam's rate of movement was 0.5-4.0 cm/s. Microstructural analysis of the treated specimens revealed both general regularities and peculiarities of the formation of the structure and substructure of the steels.

After electron beam treatment, a hardened layer with martensitic-austenitic structure was formed on the surface of all the specimens, and their structural peculiarities were conditioned by the high rates and short duration of heating. With this treatment fusion of the surface takes place with formation of a hardened zone from the liquid phase. In all the specimens, high-temperature heating led to dissolving of carbides in this zone at rates of beam movement up to 2.5 cm/s. At higher rates of movement in ShKh15 and ShKh15SG steels with an initial pearlite structure, the largest carbides do not manage to dissolve.

Structural peculiarities of the hardened layers and deeper layers of the examined specimens depending on different initial states of the metal and different electron beam parameters are presented, and their significance for the performance properties of the treated steels in bearings is discussed. Results of tests of bearings made with electron beam treated steels are presented. Principal conclusions drawn from the tests are:

1. The structure and properties of electron beam treated bearing steels depend largely on their initial structure and the composition of the carbide phase. This type of treatment is best used for hardening steel with an initial

finely dispersed structure. Maximum hardness and density of dislocations are found in the zone hardened from the solid state without full dissolving of carbides.

2. In comparison with laser treatment, electron beam treatment makes it possible to avoid decarburization of the surface layer and to obtain a more uniform structure in the beam's direction of movement as well as a thicker hardened layer.

3. To obtain bearing steels with high contact durability, it is necessary to perform electron beam treatment without the surface fusing and under conditions where carbides do not dissolve completely and a hardened layer forms.

4. Contact durability of roller bearing surfaces after electron beam treatment depends on the thickness of the secondary hardened zone. Increasing the service life of bearing surfaces is possible only if the thickness of the hardened layer exceeds by at least 50% the depth at which the zone of maximum tangential stresses from rolling lies.

Effect of the Content of Alloying Elements in Different Grades of Alloy KhN65KVMYuTB on Its High-Temperature Strength

927D0225E Moscow METALLOVEDENIYE 1
TERMICHEKAYA OBRABOTKA METALLOV
in Russian No 7, Jul 92 pp 29-31

[Article by M. A. Filatova, V. S. Sudakov, and I. V. Kabanov, Scientific and Production Association of the Central Research Institute of Machinery Manufacturing Technology, and the "Elektrostal" Plant; UDC 669.14.018.44:620.17]

[Abstract] The nickel-base alloy KhN65KVMYuTB was investigated to determine what effect the content of aluminum and titanium in different grades of it has on its high-temperature strength. In the medium grade of the alloy, the aluminum content is 1.8% and the titanium content is 1.7%, and in its high grade the percentages of these elements are 2.4 and 2.6, respectively. Thus, the combined content of Al and Ti in the alloy's chemical composition is in the range of 3-5%. As a rule, in nickel alloy production the furnace charge is calculated using the mean content of each alloying element.

Results of the investigation showed that the higher level of Al and Ti content (approximately 2.5% each) increases the alloy's long- and short-term strength as well as fatigue resistance by as much as 20% in comparison with the medium grade level, while properties that determine its workability under hot pressure treatment remain at a satisfactory level.

Deformation Waves Near Nonmetallic Inclusions in Explosive Working of Metals

927D0225F Moscow METALLOVEDENIYE 1
TERMICHEKAYA OBRABOTKA METALLOV
in Russian No 7, Jul 92 pp 32-33

[Article by S. I. Gubenko, Dnepropetrovsk Metallurgical Institute; UDC 669.14.018.298:621.9.044]

[Abstract] The effect of nonmetallic inclusions as concentrators of deformation in steel undergoing explosive working was investigated. Specimens of two brands of tempered steels were subjected to dynamic loading through the transmitting medium of a propelled plate. The microstructure and substructure of the steels near non-deforming inclusions of silicon and aluminum oxides were examined.

The investigations revealed that near nonmetallic inclusions there occur relaxation processes of a translational-rotational type having a wave character. These processes lead to the formation of complexly deformed structures in the relaxation waves. In zones of plastic relaxation the microhardness is higher than in the matrix away from inclusions. When there are several waves the microhardness of the relaxation zone is heterogeneous. Away from an Al_2O_3 inclusion 30 micrometers in size the microhardness was found to be 154 H, and in the first and second relaxation waves it was 164 and 178 H, respectively, while directly near the inclusion in the third relaxation wave, it was 189 H.

Niobium's Effect on the Structure of Chromium Ferritic Steel

927D0225G Moscow METALLOVEDENIYE 1
TERMICHEKAYA OBRABOTKA METALLOV
in Russian No 7, Jul 92 pp 35-38

[Article by G. A. Burakova, Ye. K. Koval, and M. I. Tarasyev, Dnepropetrovsk Metallurgical Institute; UDC 669.15'26'293-194]

[Abstract] The possibility of increasing the corrosion resistance of vacuum heat-treated steel used in pipes by alloying with niobium was investigated. Pipes made of 01Kh25 chromium ferritic steel, which are vacuum heat-treated, have good resistance to intercrystalline corrosion, but welds made in them are subject to this corrosion.

Steel of this brand was melted in an induction furnace and cast into 10-kg round ingots. After forging into sheet 8-10 mm thick, specimens were vacuum treated at 1300°C for 40 hours and then rolled warm to a thickness of 3 mm. Specimens with different Nb contents (0.23, 0.46 and 0.83%) were tested. The tests produced the following conclusions:

1. In 01Kh25 steel alloyed with 0.23, 0.46 and 0.83% Nb, an excess mu-phase is formed which embrittles bended specimens in tests for intercrystalline corrosion. Grain boundaries remain clean and are not subject to corrosion

failure. The steel's resistance to overall corrosion is increased by 50% when alloyed with a minimum of 0.46% Nb.

2. The presence of small particles of the mu-phase in Nb-alloyed 01Kh25 steel does not have a detrimental effect on its warm-rolling deformability.

3. The optimum Nb content for ensuring high corrosion resistance and obtaining an optimum structure for steel which undergoes vacuum heat treatment is 0.4%.

Nature of the Internal Friction Peak in Beryllium at 100-200°C

927D0225H Moscow METALLOVEDENIYE I
TERMICHESKAYA OBRABOTKA METALLOV
in Russian No 7, Jul 92 pp 38-40

[Article by G. F. Tikhinskiy, I. I. Papirova, V. M. Arzhav-
itin, B. I. Shapoval, and G. Ye. Pletenetskiy, Kharkov
Physico-Technical Institute; UDC 539.67:669.725]

[Abstract] In a number of metals whose crystal lattice has
a hexagonal close-packed structure (e.g. Zr, Zn, Be),
internal friction peaks are observed at comparatively low

temperatures (up to 300°C). To understand the nature of
this kind of peak in beryllium, the relationship of its
characteristics to the metal's purity, its structural state,
and the rate of heating of specimens and other heat
treatment parameters was investigated. Earlier investi-
gations attributed the appearance of the internal friction
peak to interaction of interstitial atoms with moving
dislocations. The present investigation did not exclude
the effect of impurities but considered it to be a sec-
ondary factor, because in beryllium at 200°C, substantial
changes in the distribution of impurities cannot take
place due to their low diffusion mobility, and thus
impurities should not by themselves cause internal fric-
tion anomalies.

Studies of the asymmetrical internal friction peak were
made in the temperature range 200-300°C using speci-
mens of polycrystalline beryllium with different levels of
purity. The results demonstrated that in the temperature
range 100-200 degrees C, internal thermal stresses are
the main cause of the appearance of the internal friction
peak in beryllium. Impurities have only an indirect
influence, acting on processes of the origin and relax-
ation of stresses.

Computer Simulation in Determining Weldability and Selecting Welding Parameters for Steels and Alloys

937D0034A Moscow SVAROCHNOYE
PROIZVODSTVO in Russian No 8, Aug 92 pp 7-9

[Article by A. N. Khakimov, Doctor of Technical Sciences, State Academy of Oil and Gas im. I. M. Gubkin; UDC 621.791.011]

[Abstract] Developments of the State Academy of Oil and Gas in the field of computerizing the work of engineers who design and make weldments are discussed. A package of applied programs for IBM PC AT computers called "Computerized Optimizer of Properties" makes it possible to determine parameters of efficient technologies for welding carbon and low-alloy steels as well as to predict the structural-phase composition and mechanical and service properties of welds, including parameters of static and cyclical crack resistance. Another development is a computerized dilatometer, KSLD-2, in which specimens are heated by the radiant energy of lamps and a system of focusing reflectors, permitting plastics, ceramics and glass to be analyzed in addition to metals. Finally, a computer-aided analyzer of pictures of weld structures was developed which consists of a PC, a high-temperature microscope, a TV camera with video control unit, and a metallography microscope. The application software for this system makes it possible to isolate individual components of a structure in black-and-white or color, to separate structural elements, and to perform statistical analyses of the accumulated parameters of structures with generation of corresponding histograms and graphs.

Resistance of Gas Mains to Propagation of Extended Continuous Fractures

937D0034B Moscow SVAROCHNOYE
PROIZVODSTVO in Russian No 8, Aug 92 pp 12-14

[Article by G. I. Makarov, Doctor of Technical Sciences, State Academy of Oil and Gas im. I. M. Gubkin; UDC 622.791.4]

[Abstract] A calculation method for evaluating the resistance of gas mains to propagation of extended continuous fractures is presented. It allows determination of parameters which contribute to inhibiting the spread of cracks and localizing damage, such as the toughness of the pipe metal and the depth of backfill covering the main. In cases where safety margins based on these parameters cannot be ensured, length and toughness requirements are calculated for crack-arrester pipes which protect at-risk sections of mains from extended damage.

Higher Durability for Large Welded Metalwork Subject to Corrosive Environments of the Oil and Gas Industry

937D0034D Moscow SVAROCHNOYE
PROIZVODSTVO in Russian No 8, Aug 92 pp 20-21

[Article by A. I. Korolev and A. V. Muradov, Candidates of Technical Sciences; UDC 621.791:622.276.05]

[Abstract] Developments of the "Antikor" International Scientific and Training Center at the State Academy of Oil and Gas aimed at improving the corrosion resistance of weldments are reviewed. They include alloyed oxide coatings with a high resistance to a number of corrosive agents for protecting valves and pump and compressor piping, and a composite polymer coating with a titanium filler for protecting lids and bottoms of tanks. With a thickness of 110-120 micrometers, the polymer coating has a hardness of 0.91-0.94 and an adhesive strength of 0.26 MPa. Unlike a number of polymer coatings, it does not accumulate static electricity.

To improve the durability of welds in unalloyed low-carbon steel subject to corrosive environments, research was performed to find ways of making welds less electrochemically heterogeneous. It was found that in aerated environments, this can be achieved by alloying the weld metal with elements which possess a higher electrochemical potential as compared with iron (e.g., nickel or copper), or which provide a more homogeneous structure (titanium), or which have both effects (molybdenum). In hydrogen sulfide-containing environments, higher corrosion resistance of welds can be achieved by reducing the carbon content in comparison with the primary metal. On the basis of the research and industrial testing of its results, recommendations have been prepared for selecting welding materials which increase the corrosion resistance of pipeline welds at oil and gas fields.

Effect of Laser Treatment on Corrosion Resistance of Steels and Welds

937D0034F Moscow SVAROCHNOYE
PROIZVODSTVO in Russian No 8, Aug 92 pp 25-28

[Article by R. D. Radchenko, Candidate of Technical Sciences, State Academy of Oil and Gas im. I. M. Gubkin; UDC 621.791.72:621.375.826]

[Abstract] Laser treatment of low-carbon steels and of welds in them was combined with subsequent heat treatment in a furnace to determine whether surface layers could be produced with enhanced corrosion-mechanical properties in hydrogen sulfide-containing environments. The steels examined were four low-carbon, low-alloy steels of the ferrite-pearlite class, and welds made by automatic arc and electroslag welding in two of these steels were also examined.

It was found that the laser treatment combined with heat treatment forms an optimum structure in surface layers with high corrosion-mechanical properties in hydrogen sulfide-containing environments. In the course of the follow-up heat treatment in a furnace, martensitic structures break up and a layer of recrystallized ferrite is formed with finely dispersed carbides which are uniformly distributed throughout the body of the grain. Laser treatment initiates the recrystallization process as a result of decarburization of the

surface. A surface layer with a recrystallized ferrite structure 100-1000 micrometers deep increases corrosion-mechanical strength under static loading in an environment of NACE. The highest stability of properties is found in a surface 500-700 micrometers deep.

It was also found that laser treatment of welds in Cr-Ni steels increases resistance to inter-crystallite corrosion in highly oxidizing environments as a result of austenization of surface layers.

END OF

FICHE

DATE FILMED

23 SEPT 1993